Atmos. Meas. Tech. Discuss., https://doi.org/10.5194/amt-2017-461
Manuscript under review for journal Atmos. Meas. Tech.
Discussion started: 22 January 2018

Atmospheric Measurement Techniques Discussions

Validation of the IASI FORLI/Eumetsat ozone products using satellite (GOME-2), ground-based (Brewer-Dobson, SAOZ) and ozonesonde measurements

Anne Boynard[1,2], Daniel Hurtmans[3], Katerina Garane[4], Florence Goutail[1], Juliette Hadji-Lazaro[1], Maria Elissavet Koukouli[4], Catherine Wespes[3], Arno Keppens[5], Jean-Pierre Pommereau[1], Andrea Pazmino[1], Dimitris Balis[4], Diego Loyola[6], Pieter Valks[6], Pierre-François Coheur[3], and Cathy Clerbaux[1,3]

[1]LATMOS/IPSL, UPMC Univ. Paris 06 Sorbonne Universités, UVSQ, CNRS, Paris, 75252, France
[2]SPASCIA, Ramonville-Saint-Agne, 31520, France
[3]Université libre de Bruxelles, Atmospheric Spectroscopy, Service de Chimie Quantique et Photophysique, Brussels, 1050, Belgium
[4]Laboratory of Atmospheric Physics, Aristotle University of Thessaloniki, Thessaloniki, 54124, Greece
[5]Royal Belgian Institute for Space Aeronomy (BIRA-IASB), Brussels, 1180, Belgium
[6]Institut für Methodik der Fernerkundung (IMF), Deutsches Zentrum für Luft- und Raumfahrt (DLR), Oberpfaffenhofen, Germany

Correspondence to: Anne Boynard (anne.boynard@latmos.ipsl.fr)

Abstract. This paper assesses the quality of IASI/Metop-A (IASI-A) and IASI/Metop-B (IASI-B) ozone (O_3) products (total and partial O_3 columns) retrieved with the Fast Optimal Retrievals on Layers for IASI Ozone (FORLI-O_3) v20151001 software for nine years (2008 – 2017) through an extensive inter-comparison and validation exercise using independent observations (satellite, ground-based and ozonesonde). IASI-A and IASI-B Total O_3 Columns (TOCs) are generally consistent, with a global mean difference less than 0.3% for both day- and nighttime measurements, IASI-A being slightly higher than IASI-B. A global difference less than 2.4 % is found for the tropospheric (TROPO) O_3 column product (IASI-A being lower than IASI-B), which is partly due to a temporary issue related to IASI-A viewing angle in 2015. Our validation shows that IASI-A and IASI-B TOCs are consistent with GOME-2, Dobson, Brewer and SAOZ retrieved ones, with global mean differences in the range 0.1 – 2 % depending on the instruments. The IASI-A and ground-based TOC comparison for the period 2008 – July 2017 shows good long-term stability (negative trends within ±3 % decade^{-1}). The comparison results between IASI-A and IASI-B against smoothed ozonesonde partial O_3 columns vary in altitude and latitude, with maximum standard deviation for the 300-150 hPa column (20-40 %) due to strong ozone variability and *a priori* uncertainty. The worst agreement with the ozonesondes and with UV-vis retrieved TOC [satellite and ground] is found at the southern high latitudes. Compared to ozonesonde data, IASI-A and IASI-B O_3 products overestimate the O_3 abundance in the stratosphere (up to 20 % for the 150-25 hPa column) and underestimates the O_3 abundance in the troposphere (within 10 % for the mid-latitudes and ~18 % for the tropics). Based on the period 2011-2016, non-significant drift is found for the northern hemispheric tropospheric columns while a small drift prevails for the period before 2011.

Atmos. Meas. Tech. Discuss., https://doi.org/10.5194/amt-2017-461
Manuscript under review for journal Atmos. Meas. Tech.
Discussion started: 22 January 2018

Atmospheric Measurement Techniques Discussions

1 Introduction

Ozone (O_3) plays a major role in the chemical and thermal balance of the atmosphere. In the stratosphere, O_3 protects the biosphere and humans from harmful ultraviolet (UV) radiation. In the troposphere, O_3 plays different important roles depending on the altitude region. Near the surface, ozone in excessive amount is one of the main air pollutants impacting both human health (Brunekreef and Holgate, 2002; Lim et al., 2012) and ecosystems (Fowler et al., 2009). In the upper troposphere, ozone is an important anthropogenic greenhouse gas (IPCC, 2013) and acts as a short-lived climate forcer (Shindell et al., 2012). Tropospheric O_3 originates either from complex photochemical reactions involving nitrogen oxides (NO_x), carbon monoxide (CO) and hydrocarbons (e.g. Chameides and Walker, 1973; Crutzen, 1973) or from the stratosphere by downward transport to the troposphere especially at mid- and high latitudes (e.g. Holton et al., 1995). The lifetime of tropospheric ozone varies with altitude and ranges from 1-2 days in the boundary layer where dry deposition is the major sink to several weeks in the free troposphere, so that the transport scale of O_3 can be intercontinental and hemispheric (Monks et al., 2015). To better understand its variability and impacts, it is therefore crucial to obtain information on its vertical, spatial and temporal distribution. These can be provided by observations from space-borne instruments.

The Infrared Atmospheric Sounding Interferometer (IASI) is a nadir-viewing spectrometer flying on board the Eumetsat's (European Organisation for the Exploitation of Meteorological Satellites) Metop-A and Metop-B satellites, since October 2006 and September 2012 respectively. In order to ensure the continuity of IASI observations for atmospheric composition monitoring, a third satellite (Metop-C) is scheduled to be launched in September 2018. Thanks to the nadir geometry complemented by off-nadir measurements up to 48.3° on both sides of the satellite track (swath of about 2200 km), each IASI instrument covers the globe twice a day, with a field of view of 4 pixels of 12 km in diameter on the ground at nadir. The two Metop satellites are on the same orbit with Equator crossing times of 09:30 (21:30) local mean time solar time for the descending (ascending) part of the orbit, and with a 180° shift. There are therefore numerous common observations between two consecutive tracks but a ~50 min temporal difference between both instruments (one satellite might be before or after the other); thus the observations are never quite simultaneous. In addition, the geometry of the observations is different and generally off-nadir with opposite angles, so the location of the observation between the two instruments varies and thus the pixels are not absolutely geographically co-localized.

Having a twice daily coverage and a 12-km diameter footprint at nadir, IASI has the potential for providing measurements for O_3 globally, with a high spatial resolution. Previous studies have demonstrated the ability of IASI to measure O_3 separately in the stratosphere (Scannell et al., 2012; Gazeaux et al., 2013), in the upper troposphere and lower stratosphere (UTLS) (e.g. Barret et al., 2011; Wespes et al., 2016), and in the troposphere (e.g. Eremenko et al., 2008; Dufour et al., 2010, 2015; Safieddine et al., 2013, 2014). Using the long-term IASI O_3 record, interannual variability of tropospheric ozone long-term trends can be derived (Safieddine et al., 2016; Wespes et al., 2016; Gaudel et al., submitted to Elementa). Lately, Wespes et al. (2017a and 2017b) analyzed eight years of IASI O_3 data to identify the main geophysical drivers (e.g., solar

flux, the Quasi-Biennial Oscillation, North Atlantic Oscillation, El Niño-Southern Oscillation) of O_3 regional and temporal variability.

Several research groups have developed O_3 retrieval algorithms for IASI based on different approaches (e.g. Barret et al., 2011; Dufour et al., 2012; Hurtmans et al., 2012; Oetjen et al., 2016). In particular, ULB & LATMOS have developed the Fast Optimal Retrievals on Layers for IASI O_3 (FORLI- O_3) software (Hurtmans et al., 2012), which uses the IASI Level-1C data to retrieve Level-2 O_3 products. A series of validation exercises of IASI O_3 products retrieved from different versions of FORLI- O_3 (v20100825, v20140922), focusing on a particular region and/or relatively short period of time were undertaken (e.g. Dufour et al., 2012; Pommier et al., 2012; Scannell et al., 2012; Gazeaux et al., 2013; Safieddine et al., 2016). Boynard et al. (2016) performed an extensive validation of IASI O_3 products retrieved from FORLI-O_3 v20140922 against a series of independent observations, on the global scale, for the period 2008 – 2014. This study reported that, on average, FORLI-O_3 v20140922 overestimates the ultraviolet (UV) Total Ozone Column (TOC) by 2-7% with the largest differences found at high latitudes. The comparison with ozonesonde vertical profiles shows that on average FORLI-O_3 v20140922 underestimates O_3 by ~5-15% in the troposphere while it overestimates O_3 by ~10-40% in the stratosphere depending on the latitude.

Several algorithm improvements were introduced later in FORLI-O_3, including absorbance look-up tables recalculated to cover a larger spectral range using the 2012 HITRAN spectroscopic database (Rothman et al., 2013), with additional numerical corrections. Boynard et al. (2016) evaluated 10 days of the new IASI O_3 products retrieved from FORLI v20151001 and found a correction of ~4% for the TOC positive bias when compared to the UV ground-based and satellite observations, bringing the overall global comparison to ~1-2% on average. It was shown that this improvement is mainly associated with a decrease in the retrieved O_3 concentration in the middle stratosphere (MD, above 30 hPa/25 km). This O_3 retrieval algorithm (FORLI-O_3 v20151001) is currently being implemented into the Eumetsat processing facility under the auspices of the Ozone and Atmospheric Composition Monitoring Satellite Application Facility (AC SAF) project in order to operationally distribute Level-2 IASI O_3 profiles to users through the EumetCast system in 2018.

In this paper, we assess the quality of the IASI O_3 products retrieved using FORLI-O_3 v20151001 (hereafter referred as to "IASI O_3 products"), with GOME-2 also on Metop, ground-based network data (Brewer, Dobson, SAOZ) and ozonesonde measurements. Section 2 briefly describes the IASI O_3 retrievals. Section 3 presents the intercomparaison between IASI-A and IASI-B O_3 derived total and tropospheric columns. Section 4 provides the IASI-A and IASI-B TOC product validation results using independent satellite and ground-based (GB) observations. The validation results of IASI partial O_3 columns against ozonesonde measurements are presented in Section 5. Finally, Section 6 summarizes the results from this new validation.

Atmos. Meas. Tech. Discuss., https://doi.org/10.5194/amt-2017-461
Manuscript under review for journal Atmos. Meas. Tech.
Discussion started: 22 January 2018

Atmospheric Measurement Techniques Discussions

2 IASI Ozone retrievals

Ozone retrievals are performed in the 1025 – 1075 cm^{-1} spectral range using the optimal estimation method (OEM) (Rodgers, 2000) and tabulated absorption cross-sections at various pressures and temperatures to speed up the radiative transfer calculation. The ozone climatology by McPeters et al. (2007) is used as *a priori* information consisting in one single O_3 *a priori* profile and variance-covariance matrix. The Eumetsat Level-2 data (pressure, water vapor, temperature and clouds) are used as input in FORLI. It is worth mentioning that the Eumetsat dataset is not homogenous since it has been processed using different versions of the IASI Level-2 Product Processing Facility between 2008 (v4.2) and 2016 (v6.2), as summarized in Van Damme et al. (2017). The error budget of the retrieved O_3 profile shows that the dominant errors originate from the limited vertical sensitivity, from the measurement noise and from uncertainties in the fitted (water vapor column) or fixed (e.g. surface emissivity, temperature profile) parameters (Hurtmans et al., 2012). In order to avoid cloud contaminated scenes, retrievals are only performed for clear or almost-clear scenes with a fractional cloud cover below 13%, identified using the cloud information from the Eumetsat operational processing (August et al., 2012). In addition, no retrieval is performed for pixels characterized by an error related to the Level-1C IASI data, by no Level-2 Eumetsat data associated with Level-1C data or by missing temperature, water vapor, surface pressure or cloud value in Level-2 Eumetsat data.

The IASI O_3 dataset used in this paper covers the period January 2008 – July 2017. The O_3 product is a vertical profile given as partial columns in molecules cm^{-2} in 40 layers between the surface and 40 km, with an extra layer from 40 km to the top of the atmosphere. It also includes other relevant information such as quality flags, *a priori* profile, total error profile and the averaging kernel matrix, on the same vertical grid. The following quality flags were applied to filter the dataset for further validation analysis. Specifically the data were excluded when: (i) the spectral fit residual root mean square error (RMS) is higher than 3.5×10^{-8} W cm^{-2} sr cm^{-1}, reflecting a too large difference between observed and simulated radiances; (ii) the spectral fit residual biased is lower than -0.75 x 10^{-9} W/(cm^2 sr cm^{-1}) or higher than 1.25 x 10^{-9} W/(cm^2 sr cm^{-1}); (iii) the partial O_3 column is negative; (iv) there were abnormal averaging kernel values; (v) the spectral fit diverged; and (vi) the total error covariance matrix is ill conditioned; (vi) the O_3 profiles have an unrealistic C-shape, with a ratio of the surface – 6 km column to the total column higher or equal to 0.085 (which indicates too high ozone in the lower troposphere, e.g. over desert due to emissivity issue); and (viii) the DOFS is lower than 2, which are mostly associated with bad quality data in the Antarctic region.

A representative IASI-A averaging kernel matrix is illustrated in Fig. 1a, showing the difficulty to distinguish the ozone structures between one level and another. However, it shows the altitude ranges characterized by peaks of sensitivity: ~5, 12, 18 and 40 km. Another way to visualize the AK matrix is to represent the AK rows as a function of altitude as shown in Fig. 1b. The AK rows are not maximal at their nominal altitudes, which indicates that other altitudes contribute to ozone value at individual retrieval altitude. A way to estimate the vertical resolution of IASI O_3 profiles is to analyze the DOFS as

a function of altitude, which it presented in Fig. 1c. The cumulative DOFS is continuously increasing with altitude, which indicates that there exists information content in the observation for the entire altitude range.

3 Intercomparison between IASI-A and IASI-B O_3 products

The comparison between IASI-A and IASI-B O_3 products is performed for the period May 2013 – July 2017. We first calculate the daily IASI-A and IASI-B averages over a 1°x1° grid. Then we calculate the monthly averaged data from the daily gridded data. A statistical analysis of IASI-A and IASI-B TOCs and tropospheric O_3 columns (referred as TROPO O_3 columns in the following) as defined by the column integrated between the surface and 300 hPa is performed with respect to time and latitude.

Figure 2 illustrates the relative differences between IASI-A and IASI-B data for 1° zonal monthly mean TOCs (computed from daily gridded data) for daytime measurements (left panel) and nighttime measurements (right panel). IASI pixels are considered as daytime or nighttime data if the solar zenith angle (SZA) is <90° or >=90°, respectively. An excellent agreement between both IASI-A and IASI-B TOCs is observed, with differences generally within 0.4 %, except for the polar regions. As already discussed in Boynard et al. (2016), a possible reason for the larger differences in polar regions is the combination of the overlap by consecutive orbits with different times and thus, different meteorological conditions. Metop, with its polar orbit, makes 14 revolutions per day, and will therefore pass by the poles on each revolution. This leads to a larger number of observations over the poles each day at different local times for the same grid cell. The variability in O_3 is therefore much larger leading to both larger differences between the measurements and larger standard deviation (not shown). Two interesting features that come out of the figure are (i) the slight increase in the differences in 2015 (April-September) and the decrease in the differences between the period prior to April 2015 and the period posteriori to October 2015. These two points will be discussed hereafter.

Figure 3 illustrates the relative differences between IASI-A and IASI-B data for 1° zonal monthly mean TROPO O_3 columns (computed from daily gridded data) for daytime measurements (left panel) and nighttime measurements (right panel). In general, the differences between IASI-A and IASI-B TROPO O_3 columns are within ±2 % although larger differences can be found locally, especially in the polar regions. As for the TOCs product, the differences decrease from October 2015 with respect to the period May 2013 – April 2015 and the differences are significantly larger for the period April – September 2015 (up to 10 %). Another noticeable feature during the period April – October 2015 is the opposite signs between the differences in TOCs (Fig. 2) and in TROPO (Fig. 3) O_3 columns.

The reason for these unexpected differences lies in the fact that on 13 April 2015, there was an error in the IASI-A pixel registration, which slightly modified the IASI-A viewing angle. This was corrected only in September 2015 and produced a 6-month period (between April and September 2015) with somewhat larger differences observed between IASI-A and IASI-B O_3 products between April and September 2015. Furthermore, on 7 October 2015, the mechanism of compensation of

IASI's corner cube mirror movements, which was proved to generate micro-vibrations and random errors in the IASI spectra was stopped. Since then, the IASI-A and IASI-B spectra are of excellent agreement.

Because of the changes made in the IASI-A Level-1 data processing, the comparison statistics are performed over two periods, excluding the period between April and September 2015: For the period May 2013 – March 2015, IASI-A TOC product measures 0.3±1.1 % less ozone than IASI-B for both day- and nighttime measurements. As expected, the overall differences and standard deviation are smaller from October 2015: IASI-A TOC product gives 0.1±0.5 % less ozone than IASI-B. Similar results are found for the TROPO O_3 column: IASI-A TROPO O_3 product gives 2.4±0.5 % and 2.1±0.4 % less than ozone than IASI-B for day- and nighttime measurements, respectively. From October 2015, the overall difference between both instruments decreases and is equal to 1.4±1.3 %.

The excellent agreement between the current IASI-A and IASI-B TOC and TROPO O_3 columns (April – October 2015 excluded) allows the combined use of IASI-A and IASI-B instruments to provide homogeneous total and tropospheric ozone data with full daily global coverage measurements. However, for the period April – October 2015, only IASI-B O_3 products should for the time being preferentially be used.

Nine years (2008-2017) of IASI-A TOC and TROPO O_3 column measurements are presented in Fig. 4 to illustrate the interannual variability of TOCs and TROPO O_3 columns. Similarities for both products are apparent among the nine years, although the amount of ozone at any one location can vary from one year to another.

4 Validation of IASI-A and IASI-B total ozone columns

4.1 Comparison with GOME-2 retrievals

The Global Ozone Monitoring Experiment-2 (GOME-2) instrument, also on board the Metop-A and B platforms, is a UV-vis-NIR (visible-near IR) nadir viewing scanning spectrometer, with an across-track scan time of 6 s and a nominal swath width of 1920 km, providing global coverage of the sunlit part of the atmosphere almost within 1.5 days (Hassinen et al., 2016; Munro et al., 2016). GOME-2 ground pixels have a footprint size of 80 km x 40 km, which is larger than that of IASI (pixel of 12 km diameter). In the framework of the Eumetsat AC SAF project, GOME-2 total ozone data are processed at DLR operationally, both in near-real time and offline, using the GOME Data Processor (GDP) algorithm (Loyola et al., 2011; Hao et al., 2014; Valks et al., 2014). The GOME-2 products has been validated using ground-based measurements (e.g Loyola et al., 2011; Koukouli et al., 2012, 2015; Hao et al., 2014), which has shown an overall agreement within 1% in most situations. As shown in Hao et al. (2014), there is an excellent agreement between the GOME-2A and GOME-2B TOCs, with a mean difference of around 0.5%. Therefore in this study the IASI-A and IASI-B validation is limited to the comparison with GOME-2A TOC products only. In this comparison we only use GOME-2A TOC data meeting the valid conditions given in Valks et al. (2017): TOC value ranging between 75 and 700 DU and slant column error low than 2 %.

Atmos. Meas. Tech. Discuss., https://doi.org/10.5194/amt-2017-461
Manuscript under review for journal Atmos. Meas. Tech.
Discussion started: 22 January 2018

The comparison between IASI-A and IASI-B against GOME-2A TOCs is not straightforward since the pixels are not co-localized in time and space, and IASI and GOME-2 instruments have different pixel size. In order to compare collocated data, a simple way is to calculate the daily average of IASI-A, IASI-B and GOME-2A TOCs along with the relative difference associated (calculated as 100 x (IASI-A - GOME-2) / GOME-2) [%], over a constant 1°x1° grid. As the UV-vis instrument provides daytime observations, only the IASI daytime data (SZA < 90°) are used in this comparison.

Figure 5 illustrates the relative differences between IASI-A and GOME-2A TOC data for 1° zonal monthly mean TOCs (computed from daily data) for the period 2008 – 2017 with their associated standard deviation. A good agreement between both TOC products is observed, with the lowest differences found in the mid-latitudes and tropics and the largest differences found in the polar regions, especially over Antarctica (difference more than 5 %). Compared to GOME-2A, IASI-A TOCs are lower in the tropics (by 0.5-07 %) and are higher in the mid-latitudes (by 0.8-1.1 %). Overall, IASI-A TOC product are slightly lower than GOME-2A TOC product, with a global mean bias of -0.5±1.5 %. Figure 6 shows the seasonal distributions of relative differences between IASI-A and GOME-2A TOCs, computed from collocated daily gridded data for the period 2008-2017 (see Table 1 for the statistics associated). The lowest differences are found in the northern mid-latitudes during summer (June-July-August) while the largest differences are found over Antarctica and Greenland, especially during the March-April-May season (3.5 % over Antarctica). The detailed analysis undertaken for different latitude bands given in Table 1 shows that the highest correlation coefficients are found in the mid-latitudes and the northern high latitudes, with values higher than 0.93. Lower correlation is found between IASI-A and GOME-2A TOCs in the Southern high latitudes during MAM (0.62) and in the tropics during SON (0.55). However, during the O_3 hole season, high correlation of 0.94 is found in the southern polar region, with IASI-A TOCs being negatively biased (~2%). This suggests that IASI-A TOC overestimates the extent of O_3 depletion (i.e. the TOCs in the ozone hole) with respect to GOME-2A TOC. As suggested in Boynard et al. (2016), possible reasons for the larger discrepancies observed at high latitudes are i) the limited information content in the IASI observations in these regions due to low surface temperatures, ii) a misrepresentation of the emissivity above ice surfaces, iii) the temperature profiles used in FORLI-O_3 that are less reliable at high latitudes and over elevated terrain as shown in August et al. (2012), and iv) the errors associated with TOC retrievals in the UV-vis spectral range increasing at high solar zenith angles in these regions, mostly because of the larger sensitivity of the retrieval to the *a priori* O_3 profile shape (Lerot et al., 2014). Further investigation would be needed to understand the reasons of these larger differences at high latitudes.

Figure 7 illustrates the time series of the monthly mean relative difference between IASI-A and IASI-B against GOME-2A TOCs along with the standard deviation for the Northern Hemisphere (NH) and Southern Hemisphere (SH). There is a pronounced seasonality in the difference between IASI-A and IASI-B against GOME-2A TOCs in the SH, with the largest differences being found during austral summer (up to 4 %) and the lowest differences during the austral winter. Compared to GOME-2A data, IASI-A (IASI-B) TOC shows less O_3 in the NH by 0.14±0.73% (0.07±0.67%) and more O_3 in the SH by 0.48±1.51% (0.36±1.98%). These results show a better agreement between IASI-A and IASI-B against GOME-2A TOC products, globally and locally, than with the previous IASI O_3 product version based on FORLI v20140922. This is due to an

update in the FORLI-O_3 algorithm but also to the use of new quality flags mostly rejecting bad quality data over deserts and Antarctica.

Figure 8 illustrates the variation of total ozone with latitude and season averaged over 9 years between 2008 and 2017 as derived from IASI-A and GOME-2A TOCs. Overall both instruments observe similar spatial and seasonal patterns, with the largest values found at mid-high latitudes during all seasons and the lowest values found in the tropics (except for the Antarctic O_3 hole season in Sep-Oct-Nov). An asymmetry can be seen between the northern and southern hemispheric polar values (northern hemispheric polar values are largest at the pole in the early spring whereas southern hemispheric total ozone peaks between 50°S and 70°S in late austral spring). Although little seasonal change in TOC is found in the tropics compared to the polar regions, larger levels are observed in summer. The annual Antarctic O_3 depletion in the austral spring season (September-October-November) is well observed by both instruments although the magnitude differs between IASI and GOME-2.

4.2 Comparison with ground-based spectrophotometer data

Daily TOC measurements from Dobson and Brewer UV spectrophotometers available for the period 2008 – 2017 were downloaded from the World Ozone and Ultraviolet Radiation Data Centre (WOUDC, http://woudc.org). The GB stations considered in this paper (see Table A1 in Boynard et al. (2016) for a complete list of the stations) have been extensively used in a series of validation papers of satellite TOC measurements (e.g. Weber et al., 2005; Balis et al., 2007a, 2007b; Koukouli et al., 2012, 2015; Boynard et al., 2016). For the IASI-A and IASI-B TOC validation, only direct sun observations are used as ground-based reference data as they are the most reliable for both the Dobson and the Brewer spectrophotometers, the latter offering an accuracy of about 1 % at moderate solar zenith angles (e.g. Kerr et al., 2002). The coincidence criteria are set to a 50-km search radius between the satellite pixel centre and the geocolocation of the ground-based station as well as to the same day of observations. For each GB measurement, only the closest IASI-A and IASI-B measurements are kept for the comparison.

Figure 9 shows the dependency of IASI-A and IASI-B against GB measurements relative differences on latitude for the period May 2013 – July 2017. For each daily ground-based measurement a relative difference is calculated as 100 x (IASI – GB) / GB [%]. All relative differences are then separated into latitudinal bins of 10° and the mean is calculated. Very similar features between the IASI-A and IASI-B comparisons can be seen, with the Antarctic being largely overestimated (~25 %) and the northern middle latitudes driving the mean comparisons around the 0 % to 2 % level. As shown by the IASI-to-Dobson comparison (left panel), the dependency on latitude is less visible for the NH due to the much larger number of collocations compared to the SH. The comparisons with Dobson measurements show differences between 0 and 2.5 % for the entire NH and for latitudes ranging between 0° and 40°S. At latitudes lower than 40°S, the differences range between 2 and 4 %, which is partially attributed to the small number of stations, the limited sensitivity in this region (especially for latitudes lower than 60°S) and the larger TOC variability within the Southern polar vortex (Garane et al., 2017; Verhoelst et

al., 2015). A similar picture is observed for the comparison with Brewer measurements. From Figure 9 we can also notice the larger differences for the 20-30°N latitude belt (more visible for the comparison with Brewer measurements), which suggests that the IASI quality flag established to filter the high values linked with emissivity-related issues (based on the ratio of the surface-6 km column relative to the TOC) remains too loose.

According to the user requirements given in the User Requirement Document of the Ozone_cci project (van der A, 2011), the stability of the ozone measurements must be within ±3 %/decade. To illustrate the long-term stability of the IASI-A TOC products, which is essential for trend studies, we analyze the time series of the monthly relative differences between IASI-A and GB TOC for the period 2008-2017. Due to the lack of GB Brewer observations in the SH, the assessment is performed for the NH only. For each GB measurement, a daily relative difference is calculated. All the relative differences are then averaged per month. Each month includes more than 180 IASI-A-GB pairs. Additionally, the trend is considered statistically significant if its *P* value is lower than 0.05. The TOC relative differences exhibit small positive trend of 0.56±0.32 % decade^{-1} and 1.38±0.25 % decade^{-1} for the Dobson and Brewer measurements, respectively, which indicates that the IASI-A TOC products are reliable for trend studies. Fig. 10 shows a very good agreement between IASI-A and GB measurements (mean differences within 1.1 %), with an obvious seasonal variability in the differences in the Dobson comparison: the smallest differences are in summer and the largest differences in winter, which is explained by the fact the TOC measurements from Dobson spectrometers depend on the stratospheric effective temperature. We can see a similar but less pronounced seasonality effect in the Brewer comparison. This is due to the fact that, even though the principles of operation between Dobson and Brewer spectrometers do not differ significantly, TOC measurements from the two types of instruments show differences in the range of ±0.6 % due to the use of different wavelengths and the different temperature dependence for the ozone absorption coefficients (Koukouli et al., 2015; Garane et al., 2017).

4.3 Comparison with ground-based SAOZ data

The IASI-A TOCs are also compared against zenith sky UV-vis measurements obtained with the SAOZ (Système d'Analyse par Observation Zénithale; Pommereau and Goutail, 1988) instruments, which are part of the Network for the Detection of Atmospheric Composition Change (NDACC). The SAOZ TOC measurements are performed in the visible Chappuis bands between 450 and 550 nm with a medium spectral resolution of 1 nm, twice a day during twilight (sunrise and sunset) at solar zenith angle ranging between 86 and 91°. The retrieval is based on the Differential Optical Absorption Spectroscopy (DOAS) procedure (Platt, 1988). Since observations are performed at twilight, SAOZ can be operated during the whole year at all latitudes up to ±67°. At latitudes higher than the polar circle, there is no measurement during permanent night in winter and during permanent day in summer. SAOZ performances have been continuously assessed by regular comparisons with UV-vis independent observations (e.g. Hofmann et al., 1995; Roscoe et al., 1999; Hendrick et al., 2011). The SAOZ total accuracy, including the cross-section uncertainties is ~6% (Hendrick et al., 2011).

In this study, eight SAOZ stations deployed at all latitudes from the Arctic to the Antarctic (see Table 3 in Boynard et al. (2016) for their locations) are used for IASI-A TOC validation. Sunrise (sunset) SAOZ measurements are compared to collocated daytime (nighttime) IASI daily data averaged in a 300 km diameter semi-circular area located to the East (West) of the ground- based station. Since similar results are found for day and nighttime measurements, only comparisons for day time data are shown.

Figure 11 shows the temporal variation of the monthly mean relative differences between IASI-A and IASI-B against SAOZ TOCs for the eight SAOZ stations for the period 2008 – 2017 for day time measurements. For each daily SAOZ measurement, a relative difference is calculated as 100 x (IASI – SAOZ) / SAOZ [%]. All the relative differences are then monthly averaged. First, we clearly see the systematic seasonality in the differences, both of increasing amplitude with latitude. Compared to SAOZ, the IASI-A and IASI-B TOCs are biased by 0.5-2 % (~1 % monthly mean averaged standard deviation) in the tropics and mid-latitudes, and this value is increasing to about 4±3 % at inside polar circle. The results are consistent with those found for the comparison with GOME-2 along with Brewer and Dobson measurements. As also observed in Boynard et al. (2016), the 4% bias drop between Bauru and Reunion stations located at the same latitude is attributed to the larger O_3 concentration in the upper troposphere above the South American continent in contrast to the Indian Ocean, which is ignored in SAOZ retrievals (Pastel et al., 2014).

The IASI-A and SAOZ TOC relative differences show small or non-significant negative decadal trends within ±3 % for all latitude zones, except for Bauru station, which is due to SAOZ retrievals (see explanation above). This shows again that the current IASI-A TOC products are homogeneous and reliable for trend studies.

5 Validation of IASI-A and IASI-B partial ozone column products

5.1 Comparison methodology

In this section, we assess the IASI-A and IASI-B O_3 products in terms of four partial columns. IASI vertical profiles are assessed in another paper (Keppens et al., 2017). The validation of IASI-A and IASI-B O_3 partial columns is performed using ozonesonde data from the WOUDC and NOAA-ESRL (http://www.esrl.noaa.gov/gmd/dv/ftpdata.html) archives. The sondes provide measurements of O_3 up to 30-35 km with a vertical resolution of ~150 m. Only sonde measurements based on electrochemical concentration cells (ECCs), which measure the oxidation of a potassium iodine (KI) solution by O_3 (Komhyr et al., 1995), are used in this study. Their accuracy is generally good (±5 %) (Deshler et al., 2008; Smit et al., 2007) and their uncertainties are lower than other types of ozonesondes (e.g. Hassler et al., 2014; Liu et al., 2013).

When validating satellite products with ozonesondes, a range of coincidence criteria can be used to select data for the validation of satellite measurements. They are defined considering the spatial and temporal scale of the variability of the O_3 and the number of available data that has to be sufficient for statistical analysis. The coincidence criteria used in this study are the same as those defined in Boynard et al. (2016), except for the time coincidence which is slightly different in order to

be more consistent with the temporal variability of tropospheric ozone: we apply coincidence criteria of 100 km search radius and ±6 h. As the ozonesonde measurements are mainly performed in the morning (local time), this implies that most of the pixels meeting these coincidence criteria correspond to pixels of the IASI morning overpass. A total of 56 ozonesonde stations in mid-latitudes, polar and tropical regions are considered for the comparison. The location of the ozonesonde stations used in the comparison is presented in Fig. 12.

To account for the difference in vertical resolution between the two data sets, the high vertically resolved ozonesonde profiles are first interpolated on the corresponding IASI vertical grid and then degraded to the IASI vertical resolution by applying the IASI retrieval AKs and *a priori* O_3 profile according to Rodgers (2000):

$$\boldsymbol{x}_s = \boldsymbol{x}_a + \mathbf{A}(\boldsymbol{x}_{sonde} - \boldsymbol{x}_a) \quad (1)$$

where $\boldsymbol{x}_s$ is the smoothed ozonesonde profile, $\boldsymbol{x}_{sonde}$ is the measured ozonesonde profile interpolated on the IASI vertical grid (referred as "raw" ozonesonde), $\boldsymbol{x}_a$ is the *a priori* profile and **A** the IASI AK matrix. Incomplete ozonesonde profiles above ozonesonde burst altitude are filled with the *a priori* profile.

The validation exercise is performed using the same partial columns as those used in Boynard et al. (2016) since these columns contain around one piece of information, have maximum sensitivity approximately in the middle of each of the layers, and reproduce the well-known cycles related to chemical and dynamical processes characterizing these layers (Wespes et al., 2016): surface-300 hPa (TROPO), 300-150 hPa (UTLS), 150-25 hPa (LMS for Lower and Middle Stratosphere) and 25-3 hPa (MS). On average, these pressure columns correspond to the following altitude columns: surface-8 km, 8-15 km, 15-22 km 22-40 km, respectively. As ozonesonde profiles are less reliable above 10 hPa, in the following the MS column is limited to 10 hPa.

For each daily ozonesonde measurement, we first apply Eq. (1) to the raw ozonesonde profile, then we calculate the four different partial columns from all IASI-A and smoothed ozonesonde profiles meeting the coincidence criteria described previously and finally we average all IASI-A and smoothed ozonesonde partial columns. To avoid unrealistic statistics skewed by extremely low values in the UTLS O_3 columns, we filter out extreme outliers exceeding 200 % relative differences.

5.2 Comparison of partial ozone columns

In this Section, approximatively 2000 ozonesonde profiles during a period extending from May 2013 to July 2017 are used for the statistical comparison of IASI-A and IASI-B against ozonesonde O_3 product. In order to assess the latitudinal variability of IASI O_3 retrieval performance, the comparison is performed for six 30° latitude bands representative of the northern high latitudes (60-90°N), northern mid-latitudes (30-60° N), northern tropics (0-30°N), southern tropics (0-30°S), southern mid-latitudes (30-60°S) and southern high latitudes (60-90°S).

Figure 13 shows the comparison of IASI-A and IASI-B against smoothed ozonesonde for the four defined partial columns for each of the six-latitude bands during 2013 – 2017. For the TROPO O_3 columns (1st column), the mean biases and

standard deviation are within 20 %, IASI-A and IASI-B underestimating the O_3 abundance in the tropics and mid-latitudes (by ~8-13 % and ~17-20 %, respectively) and overestimating the O_3 abundance at high latitudes (by 4-5 %), compared to ozonesonde data. The correlation coefficient ranges from 0.9 in the tropics to ~0.8 at middle latitudes, and from 0.5 to 0.7 at high latitudes. The linear regression slopes are in the range 0.6 – 0.9, with lower values found at high latitudes due to the reduced retrieval sensitivity to the lower troposphere. The comparison for the UTLS O_3 columns (2nd column) shows that IASI-A and IASI-B O_3 products overestimate the O_3 abundance irrespective the latitudes, with the largest biases found in the high latitudes (33-39 %) and the lowest biases found in the southern tropics (~11.5%). The standard deviation is maximum in the UTLS in all latitude bands (compared to the other partial columns) due to strong O_3 variability and *a priori* uncertainty. The linear regression slopes are close to 1 in the polar and mid-latitude regions but are around 0.5 in the tropics, which is closely related to the small amount of O_3 in the tropical UTLS. A positive bias from IASI-A and IASI-B O_3 products is also found for the LMS (3rd column) and MS (4th column) columns. The correlation coefficients are above 0.80 for the LMS column (except at high latitudes) while they are much lower for the MS column, which can be explained by the fact that the top of the MS column is limited to 10 hPa where ozonesondes generally burst, and thus some information above this pressure level is missing (DOFS=0.4 – 0.6 as indicated on the scatter plots). Note that the mean DOFS is generally in the range 0.6 – 1.4 for the TROPO, UTLS and LMS columns, the larger DOFS being found for the LMS column.

5.3 Assessment of IASI-A long-term stability

Figure 14 shows the time series of daily IASI-A and smoothed ozonesondes TROPO O_3 columns along with the corresponding differences for six selected ozonesonde stations representative of different latitude bands for the period 2008 – 2017. For these stations, IASI-A TROPO O_3 columns are in good agreement with ozonesondes TROPO O_3 columns with overall mean differences within ±3.5 DU (±14 %) and standard deviations lower than 6 DU (14 %). The comparison is also good in the high latitudes but unlike the mid-latitudes and tropics, IASI-A O_3 products overestimates the TROPO O_3 abundance with respect to ozonesonde data (4-7 DU). As shown in Fig. 12, which presents the mean and standard deviation of the differences in Dobson Unit of TROPO O_3 columns between IASI-A and smoothed ozonesonde for each ozonesonde station for the period 2008 – 2017, we can see that the IASI-A O_3 product generally underestimates the TROPO O_3 columns except in the polar regions. IASI-A TROPO O_3 product generally exhibits good agreement with ozonesonde data at most of the stations, with mean relative difference and standard deviation within 6 DU.

Figure 15 presents the monthly relative differences between IASI-A and ozonesonde for the TROPO, UTLS, LMS and MS O_3 columns for the period 2008 – 2017 in the NH where there are sufficient collocated data to assess the temporal variation of the differences (more than 40 IASI-sonde pairs per month). For each ozonesonde measurement, a daily relative difference is calculated. All the relative differences are then monthly averaged. To avoid spurious effects due to a seasonal cycle in the differences, only time series of eight years or longer are used, which gathers a total of 20 ozonesonde stations in the NH. A main feature that arises from this figure is the pronounced seasonality in the differences between IASI-A and sonde O_3 for

the UTLS and LMS column, with the lowest differences found in summer and the largest differences found in winter. We can also see a small but apparent seasonality in the differences for the TROPO O_3 column: the IASI TROPO O_3 column generally appears less biased with respect to the ozonesondes during winter. This reflects the low sensitivity of IASI associated with low brightness temperature in the troposphere and in such situations, the IASI retrieval mostly provides the *a priori* information (see Eq. 1). The differences in the TROPO O_3 column are better than -10 % during the period 2008 – 2010 and decrease to -20 % from 2011. This feature is also visible for the MS column: the difference baseline is around the 0 % level between 2008 and 2010 but near the 4 % level from 2011.

The linear trends of the monthly mean ozone biases for each sub-column are plotted in Fig. 15 for the period 2008 – 2016 (blue line). Based on the comparison of the drift value with the 2-σ standard deviation and the *P* value (indicated on each plot), the derived trends are insignificant for the UTLS and LMS but are statistically significant for the TROPO and MS columns (~-8.5 % dec^{-1} and ~5 % dec^{-1}, respectively), which is in agreement with Keppens et al. (2017) who applied a different method based on bootstrapping technique (Hubert et al., 2016). Note that the decadal drift calculated for each individual station ranges between -13 % and -7 %, with most of the larger drifts corresponding to stations that changed their instrumentations between late 2008 and early 2010 (e.g. Naha, Sapporo and Syowa). As mentioned previously we can see two distinct periods: 2008 – 2010 and 2011 – 2016. It is worth indicating that in the end of 2010 there was a change in the processing of the Eumetsat IASI Level-2 processor (see Table 1 in Van Damme et al. (2017) for a summary of the changes in Eumsetsat Level-2 data), which is likely to induce some inconsistencies but no progressive drifts in the retrieved columns. Limiting the period to 2011 – 2016, the drift values remain insignificant for the UTLS and the LMS and no statistically significant drift is found (P value >0.47 and the value of the drift is lower than its 2-sigma standard deviation). The drift before 2011 is surprising and cannot, at this point, be traced back to the IASI-A radiances, which have proven being very stable. A possible but speculative explanation for this 3-years drift is a progressive change in surface properties or in the mean atmospheric state, which would not be reflected in the FORLI software. Further work is needed to address this particular point; it should best be undertaken, to remove other possible biases, after the reprocessing of IASI Level-1 and meteorological Level-2 data.

6 Summary

In this study, we have assessed the quality of IASI-A and IASI-B O_3 products (total and partial columns) retrieved with the FORLI v20151001 software for nine years (2008 – 2017) through an extensive inter-comparison and validation exercise using independent observations (satellite, ground-based and ozonesonde). The main findings of this work can be summarized as follow:

1. The inter-comparison between IASI-A and IASI-B TOC products for the period May 2013 – July 2017 shows that, IASI-A and IASI-B TOCs are generally consistent, with a global difference less than 0.3 % for both day- and

nighttime measurements and with IASI-A TOCs slightly higher than those of IASI-B. A similar result is found for the TROPO O_3 column: a global difference less than 2.4 % for both day- and nighttime measurements is found, IASI-A TROPO O_3 columns lower than IASI-B. Inconsistencies between both instruments were found for a limited period between April and September 2015, which are due to the change in the IASI-A viewing angle that was corrected in September 2015. This has a significant impact on the TROPO O_3 product (difference up to 10 %) but a slight impact on the TOC product (difference less than 0.8 %). The consistency between IASI-A and IASI-B O_3 products becomes better from October 2015 (differences less than 0.1 % and 1.4 % for the TOC and TROPO O_3 column product, respectively), which is due to the better quality of IASI-A and IASI-B Level-1 data because of the stop of the compensation of the cube corner movements, which proved to generate micro-vibrations and random errors.

2. With respect to GOME-2A data, IASI-A and IASI-B TOCs are in excellent agreement: they are marginally lower in the Northern Hemisphere by 0.1 % while they are higher in the Southern Hemisphere by 0.5 %. There is a pronounced seasonality in the bias in the SH, with the largest biases found during the austral summer (up to 4 %), which is due to larger differences at the southern high latitudes. With respect to Dobson and Brewer data, IASI-A and IASI-B TOC product overestimates the total O_3 abundance by ~1.1 % with an obvious seasonal variability in the differences, which is caused by the ground-based measurements (see Section 4.2 for more explanation). Finally, compared to SAOZ, IASI-A and IASI-B TOC product is biased by 1-2 % (~1 % monthly mean averaged standard deviation) in the tropics and mid-latitudes, and this value is increasing to about 2.5-4 % inside the polar circles. The time series of relative differences between IASI-A against Brewer, Dobson and SAOZ TOCs show small or insignificant negative trends within ±3 % decade^{-1} for all latitude zones, except for Bauru station (located in the southern tropics), which is due to SAOZ retrieval issue still under investigation. This demonstrates the long-term stability of the current IASI-A TOC products.

3. The comparison results between IASI-A and IASI-B against smoothed ozonesonde partial O_3 columns vary in altitude, with maximum standard deviation for the UTLS (20-40 %) column due to strong ozone variability and *a priori* uncertainty. The larger bias found in the UTLS, also found with other TIR sounders (e.g. Nassar et al., 2008; Worden et al., 2007), is not fully understood but some possible explanations are the limited IASI vertical resolution, uncertainties in the ozone line parameters or the use of inadequate *a priori* information. Further investigations need to be performed. IASI-A and IASI-B O_3 products underestimate the O_3 abundance in the troposphere (by ~10 % in the mid-latitudes and ~18 % in the tropics) and overestimates the O_3 abundance in the stratosphere (less than 15 % for the 150-25 hPa). The IASI-A to ozonesonde comparison in the Northern Hemisphere exhibits statistically insignificant trends for all sub-columns for the period 2011 – 2016, as expected from the excellent stability in the Level-1, but a weak and surprising drift for the 3-years period before 2011, which is not well understood at this point.

The IASI-A and IASI-B O_3 products (total and vertical profiles) starting in October 2007 are generated by the LATMOS and ULB in a near-real time mode using FORLI-O_3 v20151001. Both IASI-A and IASI-B O_3 products retrieved using FORLI-O_3 v20151001 are already part of the Eumetsat's AC SAF Official Validation Monitoring found in lap3.physics.auth.gr/eumetsat/ as part of the operational Eumetsat services. This O_3 retrieval algorithm (FORLI-O_3 v20151001) is currently being implemented into the Eumetsat processing facility under the auspices of the AC SAF project in order to operationally distribute Level-2 IASI O_3 data to users through the EumetCast system in 2018.

7 Data availability

The IASI O_3 data processed with FORLI-O_3 v20151001 can be downloaded from the Aeris portal (http://iasi.aeris-data.fr/O3/; Aeris, 2017). The GOME-2 O_3 data are available on the AC SAF website (http://acsaf.org; AC SAF, 2017). The ozonesonde data can be downloaded from the WOUDC database (https://doi.org/10.14287/10000008; WMO/GAW Ozone Monitoring Community, 2017a) and from the NOAA-ESRL database (http://www.esrl.noaa.gov/gmd/dv/ftpdata.html; NOAA, 2017). The Brewer and Dobson soundings can be downloaded from the WOUDC database (https://doi.org/10.14287/10000004; WMO/GAW Ozone Monitoring Community, 2017b). The SAOZ data are available at http://saoz.obs.uvsq.fr (SAOZ, 2017).

Acknowledgments

IASI is a joint mission of Eumetsat and the Centre National d'Etudes Spatiales (CNES, France). The IASI Level-1C data are distributed in near real time by Eumetsat through the EumetCast system distribution. The authors acknowledge the Aeris data infrastructure (https://www.aeris-data.fr/) for providing access to the IASI Level-1C data and Level-2 temperature data used in this study. This work was undertaken in the framework of the Eumetsat AC SAF project (http://acsaf.org/), the European Space Agency O_3 Climate Change Initiative (O3-CCI, www.esa-ozone-cci.org) and the Copernicus Climate Change (C3S). The French scientists are grateful to CNES and Centre National de la Recherche Scientifique (CNRS) for financial support. The research in Belgium is also funded by the Belgian State Federal Office for Scientific, Technical and Cultural Affairs and the European Space Agency (ESA Prodex IASI Flow project). The ozonesonde data used in this study were provided by the World Ozone and Ultraviolet Data Centre (WOUDC) and the Global Monitoring Division (GMD) of NOAA's Earth System Research Laboratory and are publicly available (see http://www.woudc.org and http://www.esrl.noaa.gov/gmd). The authors thank all those responsible for the WOUDC and GMD measurements and archives for making the ozonesonde data available. The ground-based total ozone column data used in this publication were obtained as part of WMO's Global Atmosphere Watch (GAW) and are publicly available via the WOUDC. We would like to acknowledge and warmly thank all the investigators that provide data to these repositories on a timely basis, as well as the handlers of these databases for their upkeep and quality guaranteed efforts. The authors acknowledge the European

Communities, the Région Réunion, CNRS, and Université de la Réunion for their support and contribution in the construction phase of the research infrastructure OPAT (Observatoire de la Physique de l'Atmosphère à la Réunion). OPAR is presently funded by CNRS (INSU) and Université de la Réunion, and managed by OSU-R (Observation des sciences de l'Univers à la Réunion, UMS 3365). Françoise Posny, Thierry Portafaix (LACy – UMR 8105) and Jean-Marc Metzget (UMS 3365) are also acknowledged for their management, scientific follow up and technical handling of the SAOZ and ECC observations at La Réunion.

References

AC SAF: the AC SAF GOME-2 O_3 products, available at: http://acsaf.org, last access: 30 August 2017, 2017.

Aeris: the IASI O_3 products processed with FORLI-O3 v20151001, available at: http://iasi.aeris-data.fr/O3/, last access: 22 December 2017, 2017.

August, T., Klaes, D., Schlüssel, P., Hultberg, T., Crapeau, M., Arriaga, A., O'Carroll, A., Coppens, D., Munro, R., and Calbet, X.: IASI on Metop-A: Operational Level 2 retrievals after five years in orbit, J. Quant. Spectrosc. Ra., 113, 1340-1371, doi: 10.1016/j.jqsrt.2012.02.028, 2012.

Balis, D., Lambert, J.-C., Van Roozendael, M., Spurr, R., Loyola, D., Livschitz, Y., Valks, P., Amiridis, V., Gerard, P., Granville, J., and Zehner, C.: Ten years of GOME/ERS2 total ozone data the new GOME data processor (GDP) version 4: 2. Ground-based validation and comparisons with TOMS V7/V8, J. Geophys. Res., 112, D07307, doi: 10.1029/2005JD00637, 2007b.

Balis, D., Kroon, M., Koukouli, M. E., Labow, G., Veefkind, J. P., and McPeters, R. D.: Validation of Ozone Monitoring Instrument total ozone column measurements using Brewer and Dobson spectrophotometer ground based observations, J. Geophys. Res., 112, D24S46, doi:10.1029/2007JD008796, 2007a.

Barret, B., Le Flochmoen, E., Sauvage, B., Pavelin, E., Matricardi, M., and Cammas, J. P.: The detection of post-monsoon tropospheric ozone variability over south Asia using IASI data, Atmos. Chem. Phys., 11, 9533-9548, https://doi.org/10.5194/acp-11-9533-2011, 2011.

Boynard, A., Hurtmans, D., Koukouli, M. E., Goutail, F., Bureau, J., Safieddine, S., Lerot, C., Hadji-Lazaro, J., Wespes, C., Pommereau, J.-P., Pazmino, A., Zyrichidou, I., Balis, D., Barbe, A., Mikhailenko, S. N., Loyola, D., Valks, P., Van Roozendael, M., Coheur, P.-F., and Clerbaux, C.: Seven years of IASI ozone retrievals from FORLI: validation with independent total column and vertical profile measurements, Atmos. Meas. Tech., 9, 4327-4353, https://doi.org/10.5194/amt-9-4327-2016, 2016.

Boynard, B., Clerbaux, C., Clarisse, L., Safieddine, S., Pommier, M., van Damme, M., Bauduin, S., Oudot, C., Hadji-Lazaro, J., Hurtmans, D., and Coheur, P-F.: First simultaneous space measurements of atmospheric pollutants in the boundary layer from IASI: a case study in the North China Plain. Geophys. Res. Letters., http://onlinelibrary.wiley.com/doi/10.1002/2013GL058333/abstract, 2014.

Boynard, A., Clerbaux, C., Coheur, P.-F., Hurtmans, D., Turquety, S., George, M., Hadji-Lazaro, J., Keim, C., and Meyer-Arnek, J.: Measurements of total and tropospheric ozone from IASI: comparison with correlative satellite, ground-based and ozonesonde observations, Atmos. Chem. Phys., 9, 6255–6271, doi:10.5194/acp-9-6255-2009, 2009.

Brunekreef, B., and Holgate, S. T.: Air pollution and health, Lancet, 360, 1233-1242, doi:10.1016/S0140-6736(02)11274-8, 2002.

Chameides, W. L. and Walker, J. C. G.: A photochemical theory for tropospheric ozone, J. Geophys. Res., 78, 87518760, 1973.

Clerbaux, C., Hadji-Lazaro, J., Turquety, S., George, M., Boynard, A., Pommier, M., Safieddine, S. Coheur, P.-F., Hurtmans, D., Clarisse, L., and Van Damme, M., Tracking pollutants from space: Eight years of IASI satellite observation, Comptes Rendus Geoscience, http://dx.doi.org/10.1016/j.crte.2015.06.001, 2015.

Clerbaux, C., Boynard, A., Clarisse, L., George, M., Hadji-Lazaro, J., Herbin, H., Hurtmans, D., Pommier, M., Razavi, A., Turquety, S., Wespes, C., and Coheur, P.-F.: Monitoring of atmospheric composition using the thermal infrared IASI/MetOp sounder, Atmos. Chem. Phys., 9, 6041-6054, doi:10.5194/acp-9-6041-2009, 2009.

Crutzen, P. J.: Photochemical reactions initiated by and influencing ozone in the unpolluted troposphere, Tellus, 26, 47–57, 1973.

Deshler, T., Mercer, J. L., Smit, H. G. J., Stubi, R., Levrat, G., Johnson, B. J., Oltmans, S. J., Kivi, R., Thompson, A. M., Witte, J., Davies, J., Schmidlin, F. J., Brothers, G., and Sasaki, T.: Atmospheric comparison of electrochemical cell ozonesondes from different manufacturers, and with different cathode solution strengths: The Balloon Experiment on Standards for Ozonesondes, J. Geophys. Res., 113, D04307, doi:10.1029/2007JD008975, 2008.

Dessler, A.: Chemistry and Physics of Stratospheric Ozone, International Geophysics Series, vol. 74, Academic Press, London, San Diego, 2000.

Dufour, G., Eremenko, M., Cuesta, J., Doche, C., Foret, G., Beekmann, M., Cheiney, A., Wang, Y., Cai, Z., Liu, Y., Takigawa, M., Kanaya, Y., and Flaud, J.-M.: Springtime daily variations in lower-tropospheric ozone over east Asia: the role of cyclonic activity and pollution as observed from space with IASI, Atmos. Chem. Phys., 15, 10839-10856, doi:10.5194/acp-15-10839-2015, 2015.

Dufour, G., Eremenko, M., Griesfeller, A., Barret, B., LeFlochmoën, E., Clerbaux, C., Hadji-Lazaro, J., Coheur, P.-F., and Hurtmans, D.: Validation of three different scientific ozone products retrieved from IASI spectra using ozonesondes, Atmos. Meas. Tech., 5, 611-630, doi:10.5194/amt-5-611-2012, 2012.

Dufour, G., Eremenko, M., Orphal, J., and Flaud, J.-M.: IASI observations of seasonal and day-to-day variations of tropospheric ozone over three highly populated areas of China: Beijing, Shanghai, and Hong Kong, Atmos. Chem. Phys., 10, 3787-3801, doi:10.5194/acp-10-3787-2010, 2010.

Eremenko, M., Dufour, G., Foret, G., Keim, C., Orphal, J., Beekmann, M., Bergametti, G., and Flaud, J.-M.: Tropospheric ozone distributions over Europe during the heat wave in July 2007 observed from infrared nadir spectra recorded by IASI, Geophys. Res. Lett., 35, L18805, doi:10.1029/2008GL034803, 2008.

Fiore, A. M., Jacob, D. J., Bey, I., Yantosca, R. M., Field, B. D., Fusco, A. C., and Wilkinson, J. G.: Background ozone over the United States in summer: Origin, trend, and contribution to pollution episodes, J. Geophys. Res., 107(D15), 4275, doi:10.1029/2001JD000982, 2002.

Fishman, J., Watson, C. E., Larsen, J. C., and Logan, J. A.: Distribution of tropospheric ozone determined from satellite data, J. Geophys. Res., 95, 3599–3617, 1990.

Fishman, J. and Larsen, J. C.: Distribution of total ozone and stratospheric ozone in the tropics: Implications for the distribution of tropospheric ozone, J. Geophys. Res., 92, 6627–6634, 1987.

Fowler, D., Pilegaard, K., Sutton, M. A., Ambus, P., Raivonen, M., Duyzer, J., Simpson, D., Fagerli, H., et al.: Atmospheric composition change: Ecosystems-Atmosphere interactions, Atmos. Environ., 43, 5193–5267, doi:10.1016/j.atmosenv.2009.07.068, 2009.

Garane, K., Lerot, C., Coldewey-Egbers, M., Verhoelst, T., Zyrichidou, I., Balis, D. S., Danckaert, T., Goutail, F., Granville, J., Hubert, D., Koukouli, M. E., Keppens, A., Lambert, J.-C., Loyola, D., Pommereau, J.-P., Van Roozendael, M., and Zehner, C.: Quality assessment of the Ozone_cci Climate Research Data Package (release 2017): 1. Ground-based validation of total ozone column data products, Atmos. Meas. Tech. Discuss., https://doi.org/10.5194/amt-2017-378, in review, 2017

Gaudel, A., O. R. Cooper, G. Ancellet, B. Barret, A. Boynard, J. P. Burrows, C. Clerbaux, P.-F. Coheur, J. Cuesta, E. Cuevas, S. Doniki, G. Dufour, F. Ebojie, G. Foret, O. Garcia, M. J. Granados-Muñoz, J. Hannigan, F. Hase, B. Hassler, G. Huang, D. Hurtmans, D. Jaffe, N. Jones, P. Kalabokas, B. Kerridge, S. Kulawik, B. Latter, T. Leblanc, E. Le Flochmoën, W. Lin, J. Liu, X. Liu, E. Mahieu, A. McClure-Begley, J. Neu, M. Osman, M. Palm, H. Petetin, I. Petropavlovskikh, R. Querel, N. Rahpoe, A. Rozanov, M. G. Schultz, J. Schwab, R. Siddans, D. Smale, M. Steinbacher, H. Tanimoto, D. Tarasick, V. Thouret, A. M. Thompson, T. Trickl, E. Weatherhead, C. Wespes, H. Worden, C. Vigouroux, X. Xu, G. Zeng, J. Ziemke: Tropospheric Ozone Assessment Report: Present-day distribution and trends of tropospheric ozone relevant to climate and global atmospheric chemistry model evaluation, submitted to Elementa, 2017.

Gazeaux, J., Clerbaux, C., George, M., Hadji-Lazaro, J., Kuttippurath, J., Coheur, P.-F., Hurtmans, D., Deshler, T., Kovilakam, M., Campbell, P., Guidard, V., Rabier, F., and Thépaut, J.-N.: Intercomparison of polar ozone profiles by IASI/MetOp sounder with 2010 Concordiasi ozonesonde observations, Atmos. Meas. Tech., 6, 613-620, doi:10.5194/amt-6-613-2013, 2013.

Hao, N., Koukouli, M. E., Inness, A., Valks, P., Loyola, D. G., Zimmer, W., Balis, D. S., Zyrichidou, I., Van Roozendael, M., Lerot, C., and Spurr, R. J. D.: GOME-2 total ozone columns from MetOp-A/MetOp-B and assimilation in the MACC system, Atmos. Meas. Tech., 7, 2937-2951, doi:10.5194/amt-7-2937-2014, 2014.

Hassinen, S., Balis, D., Bauer, H., Begoin, M., Delcloo, A., Eleftheratos, K., Gimeno Garcia, S., Granville, J., Grossi, M., Hao, N., Hedelt, P., Hendrick, F., Hess, M., Heue, K.-P., Hovila, J., Jønch-Sørensen, H., Kalakoski, N., Kauppi, A., Kiemle, S., Kins, L., Koukouli, M. E., Kujanpää, J., Lambert, J.-C., Lang, R., Lerot, C., Loyola, D., Pedergnana, M., Pinardi, G., Romahn, F., van Roozendael, M., Lutz, R., De Smedt, I., Stammes, P., Steinbrecht, W., Tamminen, J., Theys, N., Tilstra, L.

G., Tuinder, O. N. E., Valks, P., Zerefos, C., Zimmer, W., and Zyrichidou, I.: Overview of the O3M SAF GOME-2 operational atmospheric composition and UV radiation data products and data availability, Atmos. Meas. Tech., 9, 383-407, https://doi.org/10.5194/amt-9-383-2016, 2016.

Hassler, B., Petropavlovskikh, I., Staehelin, J., August, T., Bhartia, P. K., Clerbaux, C., Degenstein, D., Mazière, M. D., Dinelli, B. M., Dudhia, A., Dufour, G., Frith, S. M., Froidevaux, L., Godin-Beekmann, S., Granville, J., Harris, N. R. P., Hoppel, K., Hubert, D., Kasai, Y., Kurylo, M. J., Kyrölä, E., Lambert, J.-C., Levelt, P. F., McElroy, C. T., McPeters, R. D., Munro, R., Nakajima, H., Parrish, A., Raspollini, P., Remsberg, E. E., Rosenlof, K. H., Rozanov, A., Sano, T., Sasano, Y., Shiotani, M., Smit, H. G. J., Stiller, G., Tamminen, J., Tarasick, D. W., Urban, J., van der A, R. J., Veefkind, J. P., Vigouroux, C., von Clarmann, T., von Savigny, C., Walker, K. A., Weber, M., Wild, J., and Zawodny, J. M.: Past changes in the vertical distribution of ozone – Part 1: Measurement techniques, uncertainties and availability, Atmos. Meas. Tech., 7, 1395-1427, https://doi.org/10.5194/amt-7-1395-2014, 2014.

Hendrick, F., Pommereau, J.-P., Goutail, F., Evans, R. D., Ionov, D., Pazmino, A., Kyrö, E., Held, G., Eriksen, P., Dorokhov, V., Gil, M., and Van Roozendael, M.: NDACC/SAOZ UV-visible total ozone measurements: improved retrieval and comparison with correlative ground-based and satellite observations, Atmos. Chem. Phys., 11, 5975-5995, doi:10.5194/acp-11-5975-2011, 2011.

Hofmann, D. J., Bonasoni, P., De Maziere, M., Evangelisti, F., Giovanelli, G., Glodman, A., Goutail, F., Harder, J., et al.: Intercomparison of UV/visible spectrometers for measurements of stratospheric NO2 for the Network for the Detection of Stratospheric Change, J. Geophys. Res., 100, 16,765-16,791, 1995.

Holton, J. R., Haynes, P. H., McIntyre, M. E., Douglass, A. R., Rood, R. B., and Pfister, L.: Stratosphere-troposphere exchange. Rev. Geophys., 33, 403–439, 1995.

Hubert, D., Lambert, J.-C., Verhoelst, T., Granville, J., Keppens, A., Baray, J.-L., Bourassa, A. E., Cortesi, U., Degenstein, D. A., Froidevaux, L., Godin-Beekmann, S., Hoppel, K. W., Johnson, B. J., Kyrölä, E., Leblanc, T., Lichtenberg, G., Marchand, M., McElroy, C. T., Murtagh, D., Nakane, H., Portafaix, T., Querel, R., Russell III, J. M., Salvador, J., Smit, H. G. J., Stebel, K., Steinbrecht, W., Strawbridge, K. B., Stübi, R., Swart, D. P. J., Taha, G., Tarasick, D. W., Thompson, A. M., Urban, J., van Gijsel, J. A. E., Van Malderen, R., von der Gathen, P., Walker, K. A., Wolfram, E., and Zawodny, J. M.: Ground-based assessment of the bias and long-term stability of 14 limb and occultation ozone profile data records, Atmos. Meas. Tech., 9, 2497-2534, https://doi.org/10.5194/amt-9-2497-2016, 2016.

Hurtmans, D., Coheur, P.-F., Wespes, C., Clarisse, L., Scharf, O., Clerbaux, C., Hadji-Lazaro, J., George, M., and Turquety, S.: FORLI radiative transfer and retrieval code for IASI, J. Quant. Spectrosc. Ra., 113, 1391–1408, doi:10.1016/j.jqsrt.2012.02.036, 2012.

IPCC: Climate Change 2013: The Physical Science Basis: Summary for Policymakers, Cambridge, UK, 2013.

Keppens, A., J.-C. Lambert, J. Granville, D. Hubert, T. Verhoelst, S. Compernolle, B. Latter, B. Kerridge, R. Siddans, A. Boynard, J. Hadji-Lazaro, C. Clerbaux, C. Wespes, D. R. Hurtmans, P.-F. Coheur, J. van Peet, R. van der A, K. Garane, M.

E. Koukouli, D. S. Balis, A. Delcloo, R. Kivi, R. Stübi, S. Godin-Beekmann, M. Van Roozendael, C. Zehner: Quality assessment of the Ozone_cci Climate Research Data Package (release 2017): 2. Ground-based validation of nadir ozone profile data products, submitted to this QOS special issue, 2017.

Kerr, J. B.: New methodology for deriving total ozone and other atmospheric variables from Brewer spectrophotometer direct sun spectra, J. Geophys. Res., 107, 4731, doi:10.1029/2001JD001227, 2002.

Komhyr, W. D., Barnes, R. A., Brothers, G. B., Lathrop, J. A., and Opperman, D. P.: Electrochemical concentration cell ozonesonde performance evaluation during STOIC 1989, J. Geophys. Res., 100, 9231–9244, doi:10.1029/94JD02175, 1995.

Koukouli, M. E., Balis, D. S., Loyola, D., Valks, P., Zimmer, W., Hao, N., Lambert, J.-C., Van Roozendael, M., Lerot, C., and Spurr, R. J. D.: Geophysical validation and long-term consistency between GOME-2/MetOp-A total ozone column and measurements from the sensors GOME/ERS-2, SCIAMACHY/ENVISAT and OMI/Aura, Atmos. Meas. Tech., 5, 2169-2181, doi:10.5194/amt-5-2169-2012, 2012.

Koukouli, M. E., Lerot, C., Granville, J., Goutail, F., Lambert, J.-C., Pommereau, J.-P., Balis, D., Zyrichidou, I., et al.: Evaluating a new homogeneous total ozone climate data record from GOME/ERS-2, SCIAMACHY/Envisat, and GOME-2/MetOp-A, J. Geophys. Res. Atmos., 120, doi:10.1002/2015JD023699, 2015.

Lerot, C., Van Roozendael, M., Spurr, R., Loyola, D., Coldewey-Egbers, M., Kochenova, S., van Gent, J., Koukouli, M., Balis, D., Lambert, J.-C., Granville, J. and Zehner, C.: Homogenized total ozone data records from the European sensors GOME/ERS-2, SCIAMACHY/Envisat, and GOME-2/MetOp-A, J. Geophys. Res. Atmos., 119(3), 1639–1662, doi:10.1002/2013JD020831, 2014.

Lim, S. S., Vos T., Flaxman A. D., Danaei G., Shibuya K., Adair-Rohani H., Amann, M, Anderson, H. R., et al. : A comparative risk assessment of burden of disease and injury attributable to 67 risk factors and risk factor clusters in 21 regions, 1990–2010: a systematic analysis for the Global Burden of Disease study 2010, Lancet 380:2224–2260, 2012.

Liu, G., Liu, J., Tarasick, D. W., Fioletov, V. E., Jin, J. J., Moeini, O., Liu, X., Sioris, C. E., and Osman, M.: A global tropospheric ozone climatology from trajectory-mapped ozone soundings, Atmos. Chem. Phys., 13, 10659-10675, https://doi.org/10.5194/acp-13-10659-2013, 2013.

Loyola, D. G., Koukouli, M. E., Valks, P., Balis, D. S., Hao, N., Van Roozendael, M., Spurr, R. J. D., Zimmer, W., et al.: The GOME-2 total column ozone product: Retrieval algorithm and ground-based validation, J. Geophys. Res., 116, D07302, doi:10.1029/2010JD014675, 2011.

McPeters, R. D., Labow, G. J., and Logan, J. A.: Ozone climatological profiles for satellite retrieval algorithms, J. Geophys. Res., 112, D05308, doi:10.1029/2005JD006823, 2007.

Monks, P. S., Archibald, A. T., Colette, A., Cooper, O., Coyle, M., Derwent, R., Fowler, D., Granier, C., Law, K. S., Mills, G. E., Stevenson, D. S., Tarasova, O., Thouret, V., von Schneidemesser, E., Sommariva, R., Wild, O., and Williams, M. L.: Tropospheric ozone and its precursors from the urban to the global scale from air quality to short-lived climate forcer, Atmos. Chem. Phys., 15, 8889-8973, doi:10.5194/acp-15-8889-2015, 2015.

Munro, R., Lang, R., Klaes, D., Poli, G., Retscher, C., Lindstrot, R., Huckle, R., Lacan, A., Grzegorski, M., Holdak, A., Kokhanovsky, A., Livschitz, J., and Eisinger, M.: The GOME-2 instrument on the Metop series of satellites: instrument design, calibration, and level 1 data processing – an overview, Atmos. Meas. Tech., 9, 1279-1301, https://doi.org/10.5194/amt-9-1279-2016, 2016.

Nassar, R., Logan, J. A., Worden, H. M., Megretskaia, I. A., Bowman, K. W., Osterman, G. B., Thompson, A. M., Tarasick, D. W., Austin, S., Claude, H., Dubey, M. K., Hocking, W. K., Johnson, B. J., Joseph, E., Merrill, J., Morris, G. A., Newchurch, M., Oltmans, S. J., Posny, F., Schmidlin, F. J., Vomel, H., Whiteman, D. N., and Witte, J. C.: Validation of Tropospheric Emission Spectrometer (TES) nadir ozone profiles using ozonesonde measurements, J. Geophys. Res.-Atmos., 113, D15S17, doi:10.1029/2007jd008819, 2008.

NOAA: the NOAA-ESRL ozone soundings, available at: http://www.esrl.noaa.gov/gmd/dv/ftpdata.html, last access: 17 December 2017, 2017.

Oetjen, H., Payne, V. H., Neu, J. L., Kulawik, S. S., Edwards, D. P., Eldering, A., Worden, H. M., and Worden, J. R.: A joint data record of tropospheric ozone from Aura-TES and MetOp-IASI, Atmos. Chem. Phys., 16, 10229-10239, https://doi.org/10.5194/acp-16-10229-2016, 2016.

Pastel, M., Pommereau, J.-P., Goutail, F., Richter, A., Pazmiño, A., Ionov, D., and Portafaix, T.: Construction of merged satellite total O_3 and NO_2 time series in the tropics for trend studies and evaluation by comparison to NDACC SAOZ measurements, Atmos. Meas. Tech., 7, 3337-3354, doi:10.5194/amt-7-3337-2014, 2014.

Platt, U.: Differential optical absorption spectroscopy (DOAS), Chem. Anal. Series, 127, 27 - 83, 1994.

Pommereau, J.-P. and Goutail, F.: Ground-based measurements by visible spectrometry during Arctic Winter and Spring, Geophys. Res. Lett., 15, 891–894, 1988.

Pommier, M., Clerbaux, C., Law, K. S., Ancellet, G., Bernath, P., Coheur, P.-F., Hadji-Lazaro, J., Hurtmans, D., Nédélec, P., Paris, J.-D., Ravetta, F., Ryerson, T. B., Schlager, H., and Weinheimer, A. J.: Analysis of IASI tropospheric O3 data over the Arctic during POLARCAT campaigns in 2008, Atmos. Chem. Phys., 12, 7371-7389, doi:10.5194/acp-12-7371-2012, 2012.

Rodgers, C. D.: Inverse Methods for Atmospheric Sounding: Theory and Practice, World Scientific, Series on Atmospheric, Oceanic and Planetary Physics, 2, Hackensack, N. J., 2000.

Roscoe, H. K., Johnston, P. V., Van Roozendael, M., Richter, A., Sarkissian, A., Roscoe, J., Preston, K. E., Lambert, J.-C., Hermans, C., Decuyper, W., Dzienus, S., Winterrath, T., Burrows, J. P., Goutail, F., Pommereau, J.-P., D'Almeida, E., Hottier, J., Coureul, C., Didier, R., Pundt, I., Bartlett, L. M., Rothman, L., Gordon, I., Babikov, Y., Barbe, A., Benner, D. C., Bernath, P., Birk, M., Bizzocchi, L., Boudon, V., Brown, L., Campargue, A., Chance, K., Cohen, E., Coudert, L., Devi, V., Drouin, B., Fayt, A., Flaud, J.-M., Gamache, R., Harrison, J., Hartmann, J.-M., Hill, C., Hodges, J., Jacquemart, D., Jolly, A., Lamouroux, J., Roy, R. L., Li, G., Long, D., Lyulin, O., Mackie, C., Massie, S., Mikhailenko, S., Müller, H., Naumenko, O., Nikitin, A., Orphal, J., Perevalov, V., Perrin, A., Polovtseva, E., Richard, C., Smith, M., Starikova, E., Sung, K., Tashkun, S., Tennyson, J., Toon, G., Tyuterev, V., and Wagner, G.: The HITRAN2012 molecular spectroscopic database, J. Quant. Spectrosc. Ra., 130, 4–50, doi: 10.1016/j.jqsrt.2013.07.002, 2013.

Safieddine, S., Boynard, A., Hao, N., Huang, F., Wang, L., Ji, D., Barret, B., Ghude, S. D., Coheur, P.-F., Hurtmans, D., and Clerbaux, C.: Tropospheric ozone variability during the East Asian summer monsoon as observed by satellite (IASI), aircraft (MOZAIC) and ground stations, Atmos. Chem. Phys., 16, 10489-10500, https://doi.org/10.5194/acp-16-10489-2016, 2016.

Safieddine, S., Boynard, A., Coheur, P.-F., Hurtmans, D., Pfister, G., Quennehen, B., Thomas, J. L., Raut, J.-C., Law, K. S., Klimont, Z., Hadji-Lazaro, J., George, M., and Clerbaux, C.: Summertime tropospheric ozone assessment over the Mediterranean region using the thermal infrared IASI/MetOp sounder and the WRF-Chem model, Atmos. Chem. Phys., 14, 10119-10131, doi:10.5194/acp-14-10119-2014, http://www.atmos-chem-phys.net/14/10119/2014/acp-14-10119-2014.html, 2014.

Safieddine, S., Clerbaux, C., George, M., Hadji-Lazaro, J., Hurtmans, D., Coheur, P.-F., Wespes, C., Loyola, D., Valks, P. and Hao, N.: Tropospheric ozone and nitrogen dioxide measurements in urban and rural regions as seen by IASI and GOME-2. J. Geophys. Res., Atmospheres, VOL. 118, 1-12, http://onlinelibrary.wiley.com/doi/10.1002/jgrd.50669/abstract, 2013.

SAOZ: the SAOZ total ozone soundings, available at: http://saoz.obs.uvsq.fr, last access: 22 December 2017, 2017.

Scannell, C., Hurtmans, D., Boynard, A., Hadji-Lazaro, J., George, M., Delcloo, A., Tuinder, O., Coheur, P.-F., and Clerbaux, C.: Antarctic ozone hole as observed by IASI/MetOp for 2008–2010, Atmos. Meas. Tech., 5, 123-139, doi:10.5194/amt-5-123-2012, 2012.

Shindell, D., Kuylenstierna, J. C. I., Vignati, E., van Dingenen, R., Amann, M., Klimont, Z., Anenberg, S. C., Muller, N., Janssens-Maenhout, G., Raes, F., Schwartz, J., Faluvegi, G., Pozzoli, L., Kupiainen, K., Höglund-Isaksson, L., Emberson, L., Streets, D., Ramanathan, V., Hicks, K., Oanh, N. T. K., Milly, G., Williams, M., Demkine, V., and Fowler, D.: Simultaneously Mitigating Near-Term Climate Change and Improving Human Health and Food Security, Science, 335, 183–189, doi:10.1126/science.1210026, 2012.

Smit, H. G. J., Straeter, W., Johnson, B., Oltmans, S., Davies, J., Tarasick, D. W., Hoegger, B., Stubi, R., Schmidlin, F., Northam, T., Thompson, A., Witte, J., Boyd, I., and Posny, F.: Assessment of the performance of ECC-ozonesondes under quasi-flight conditions in the environmental simulation chamber: Insights from the Juelich Ozone Sonde Intercomparison Experiement (JOSIE), J. Geophys. Res., 112, D19306, doi:10.1029/2006JD007308, 2007.

Valks, P., Loyola, D., Zimmer, W., Kiemle, S., Hao, N., Hedelt, P., Grossi, M., and Pedergnana, M.: Product User Manual: GOME-2 Total Columns of Ozone, NO_2, BrO, HCHO, SO_2, H_2O, OCIO and cloud Properties, DLR, Germany, June 2017, http://acsaf.org/docs/pum/Product_User_Manual_NTO_OTO_DR_GDP48_Jun_2017.pdf.

Valks, P., Hao, N., Gimeno Garcia, S., Loyola, D., Dameris, M., Jöckel, P., and Delcloo, A.: Tropical tropospheric ozone column retrieval for GOME-2, Atmos. Meas. Tech., 7, 2513–2530, doi:10.5194/amt-7-2513-2014, 2014.

van der A, et al., User Requirement Document, Issue: 2.1 Date of issue: 21/11/2011 Reference: Ozone_cci_URD_2.1, Ozone-CCI, 2011, http://www.esa-ozone-cci.org/?q=webfm_send/37, last accessed: 10.09.2017.

Van Damme, M., Whitburn, S., Clarisse, L., Clerbaux, C., Hurtmans, D., and Coheur, P.-F.: Version 2 of the IASI NH3 neural network retrieval algorithm: near-real-time and reanalysed datasets, Atmos. Meas. Tech., 10, 4905-4914, https://doi.org/10.5194/amt-10-4905-2017, 2017.

Verhoelst, T., Granville, J., Hendrick, F., Köhler, U., Lerot, C., Pommereau, J.-P., Redondas, A., Van Roozendael, M., and Lambert, J.-C.: Metrology of ground-based satellite validation: co-location mismatch and smoothing issues of total ozone comparisons, Atmos. Meas. Tech., 8, 5039-5062, https://doi.org/10.5194/amt-8-5039-2015, 2015.

Weber, M., Lamsal, L. N., Coldewey-Egbers, M., Bramstedt, K., and Burrows, J. P.: Pole-to-pole validation of GOME WFDOAS total ozone with groundbased data, Atmos. Chem. Phys., 5, 1341-1355, doi:10.5194/acp-5-1341-2005, 2005.

Wespes, C., Hurtmans, D., Clerbaux, C., Boynard, Anne., Coheur, P.-F.: Decrease in tropospheric O3 levels of the Northern Hemisphere observed by IASI, in review, 2017b.

Wespes, C., D. Hurtmans, C. Clerbaux, and P.-F. Coheur: O3 variability in the troposphere as observed by IASI over 2008–2016 — Contribution of atmospheric chemistry and dynamics, J. Geophys. Res. Atmos., 122, 2429–2451, doi:10.1002/2016JD025875, 2017a.

Wespes, C., D. Hurtmans, L.K. Emmons, S. Safieddine, C. Clerbaux, D.P. Edwards, and P.-F. Coheur: Ozone variability in the troposphere and the stratosphere from the first six years of IASI observations (2008-2013), Atmos. Chem. Phys., 16, 5721-5743, 2016.

Worden, H. M., Logan, J. A., Worden, J. R., Beer, R., Bowman, K., Clough, S. A., Eldering, A., Fisher, B. M., Gunson, M. R., Herman, R. L., Kulawik, S. S., Lampel, M. C., Luo, M., Megretskaia, I. A., Osterman, G. B., and Shephard, M. W.: Comparisons of Tropospheric Emission Spectrometer (TES) ozone profiles to ozonesondes: Methods and initial results, J. Geophys. Res., 112, D03309, doi:10.1029/2006JD007258, 2007.

WMO/GAW Ozone Monitoring Community: World Meteorological Organization-Global Atmosphere Watch Program (WMO-GAW)/World Ozone and Ultraviolet Radiation Data Centre (WOUDC) total ozone data, available at: https://doi.org/10.14287/10000004, last access: 15 December 2017, 2017b.

WMO/GAW Ozone Monitoring Community: World Meteorological Organization-Global Atmosphere Watch Program (WMO-GAW)/World Ozone and Ultraviolet Radiation Data Centre (WOUDC) ozonesonde data, available at: https://doi.org/10.14287/10000008, last access: 30 August 2017, 2017a.

Atmos. Meas. Tech. Discuss., https://doi.org/10.5194/amt-2017-461
Manuscript under review for journal Atmos. Meas. Tech.
Discussion started: 22 January 2018

Atmospheric Measurement Techniques Discussions

Tables

Table 1. Summary of correlation (R), bias and standard deviation of IASI-A and GOME-2A TOC products, for each season of the period 2008 – 2017. The bias and the standard deviation are given in percent. The correlation coefficients lower than 0.85 are indicated in italics.

Latitude range	Dec-Jan-Feb		Mar-Apr-May		Jun-Jul-Aug		Sep-Oct-Nov	
	R	Bias (%)	R	Bias (%)	R	Bias (%)	R	Bias (%)
90°S – 90°N	0.96	-1.3±4.5	0.98	0.4±4.1	0.97	-0.8±3.8	0.93	-0.7±3.4
60 – 90°N	0.94	-2.8±5.9	0.93	-0.8±4.8	0.85	-3.4±3.7	0.88	-0.7±3.1
30 – 60° N	0.96	-3.0±3.8	0.97	-1.3±3.6	0.93	-1.2±3.3	0.90	-1.3±2.8
0 – 30° N	*0.83*	-0.6±2.7	0.86	0.6±3.7	*0.80*	1.8±2.9	*0.55*	1.0±1.7
0 – 30°S	0.86	0.2±2.5	0.82	1.1±2.3	0.89	2.0±2.5	0.87	0.9±2.5
30 – 60°S	0.94	-1.7±3.0	0.94	-0.1±2.6	0.95	-1.7±3.0	0.94	-3.2±3.3
60 – 90°S	0.94	-1.1±3.4	*0.62*	3.5±3.9	-	-	0.94	-2.1±5.2

Atmos. Meas. Tech. Discuss., https://doi.org/10.5194/amt-2017-461
Manuscript under review for journal Atmos. Meas. Tech.
Discussion started: 22 January 2018

Atmospheric Measurement Techniques Discussions

Figures

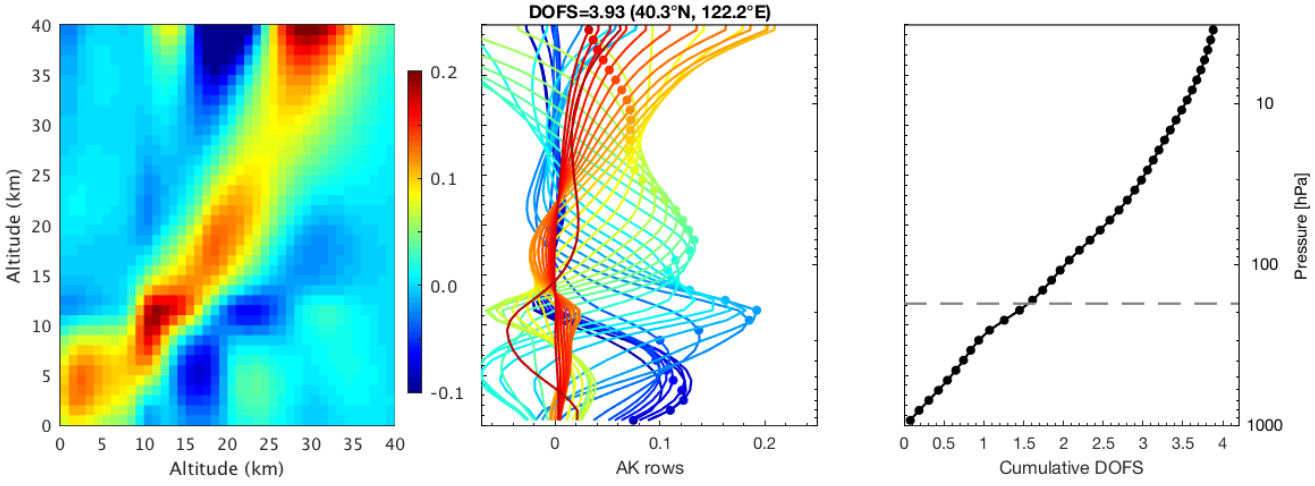

Figure 1: (left) Example of the averaging kernel matrix for the IASI-A vertical profile retrieval indicating where the information present in the IASI-A vertical ozone profile (horizontal axis) originates from in the atmosphere (vertical axis). (middle) Other representation of the averaging kernel matrix (each line is a row of the averaging kernel matrix); The nominal height of each kernel is marked by a circle. (right) cumulative DOFS obtained from the diagonal of the averaging kernel matrix. The averaging kernels expressed in (molecules cm^{-2}) / (molecules cm^{-2}) correspond to one daytime mid-latitude measurement (40.3°N, 122.2°E) obtained on 1^{rst} June 2016 for each 1 km retrieved layers from the surface to 40 k altitude.

Atmos. Meas. Tech. Discuss., https://doi.org/10.5194/amt-2017-461
Manuscript under review for journal Atmos. Meas. Tech.
Discussion started: 22 January 2018

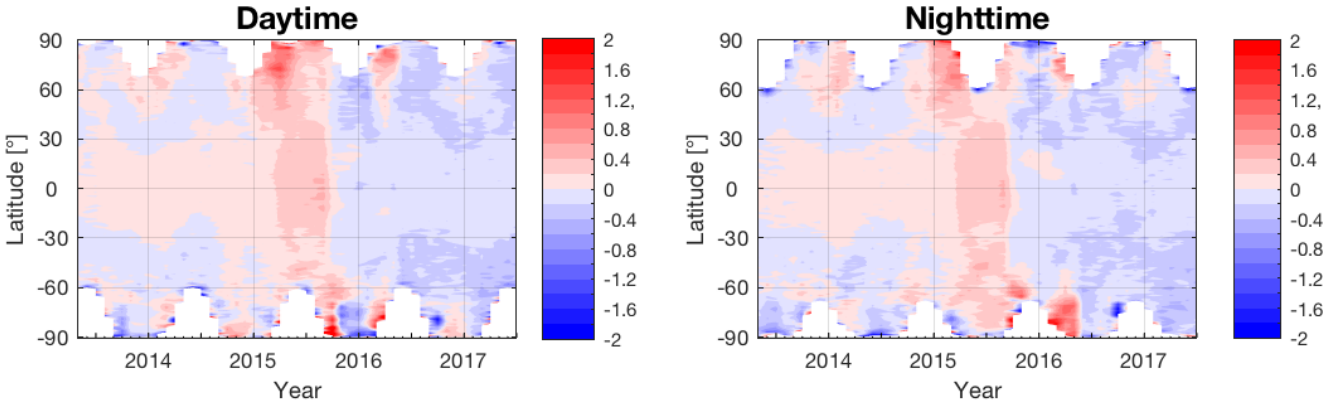

Figure 2: Contour representation of the relative difference (in percent) between IASI-A and IASI-B Total Ozone Column (TOC) products for 1° zonal monthly mean TOCs for the period May 2013 – July 2017 for daytime data (left) and nighttime data (right). The relative differences are calculated as 100 x (IASI-A - IASI-B) / IASI-A.

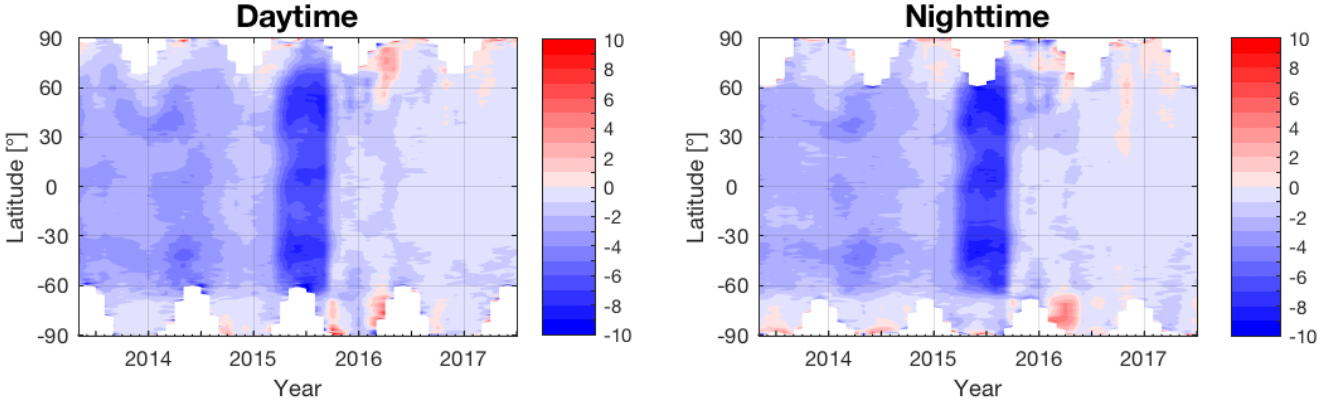

Figure 3: Same as Fig. 2 for the TROPO O_3 column products (defined as the column integrated between the surface and 300 hPa).

Atmos. Meas. Tech. Discuss., https://doi.org/10.5194/amt-2017-461
Manuscript under review for journal Atmos. Meas. Tech.
Discussion started: 22 January 2018

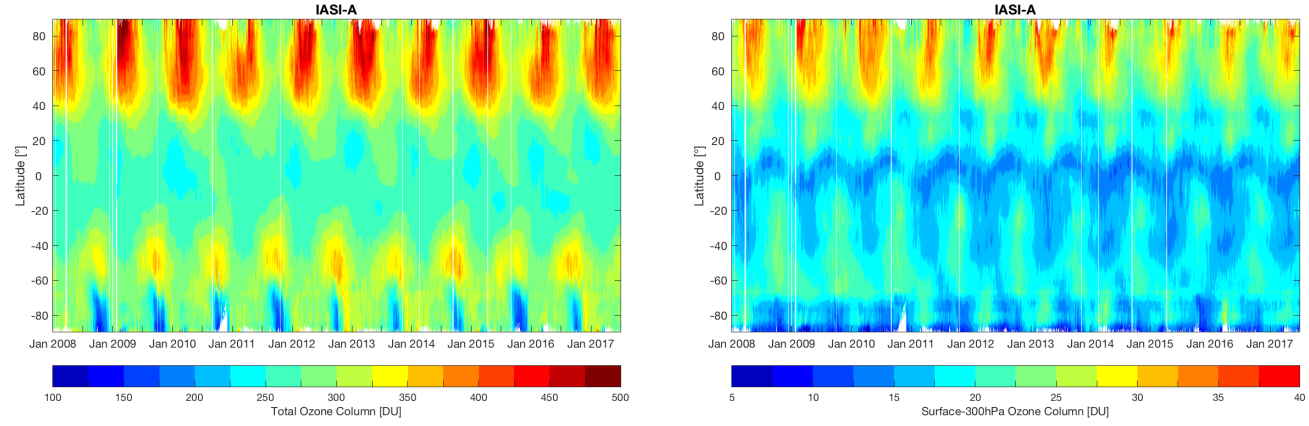

Figure 4 IASI-A Total Ozone Column (left) and TROPO O_3 column (right) record as a function of latitude and time from January 2008 to July 2017. The TROPO O_3 column is calculated as the column integrated between the surface and 300 hPa and is expressed in Dobson Unit (DU).

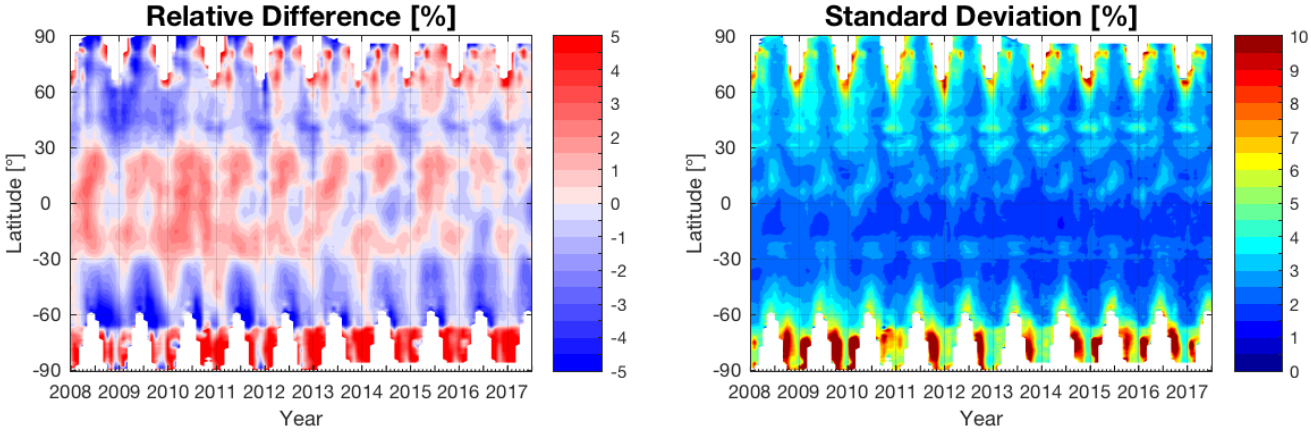

Figure 5: (left) Relative differences (in percent) between IASI-A and GOME-2A for 1° zonal monthly mean Total Ozone Columns during the period 2008 – 2017; (right) Associated standard deviation (in percent).

Atmos. Meas. Tech. Discuss., https://doi.org/10.5194/amt-2017-461
Manuscript under review for journal Atmos. Meas. Tech.
Discussion started: 22 January 2018

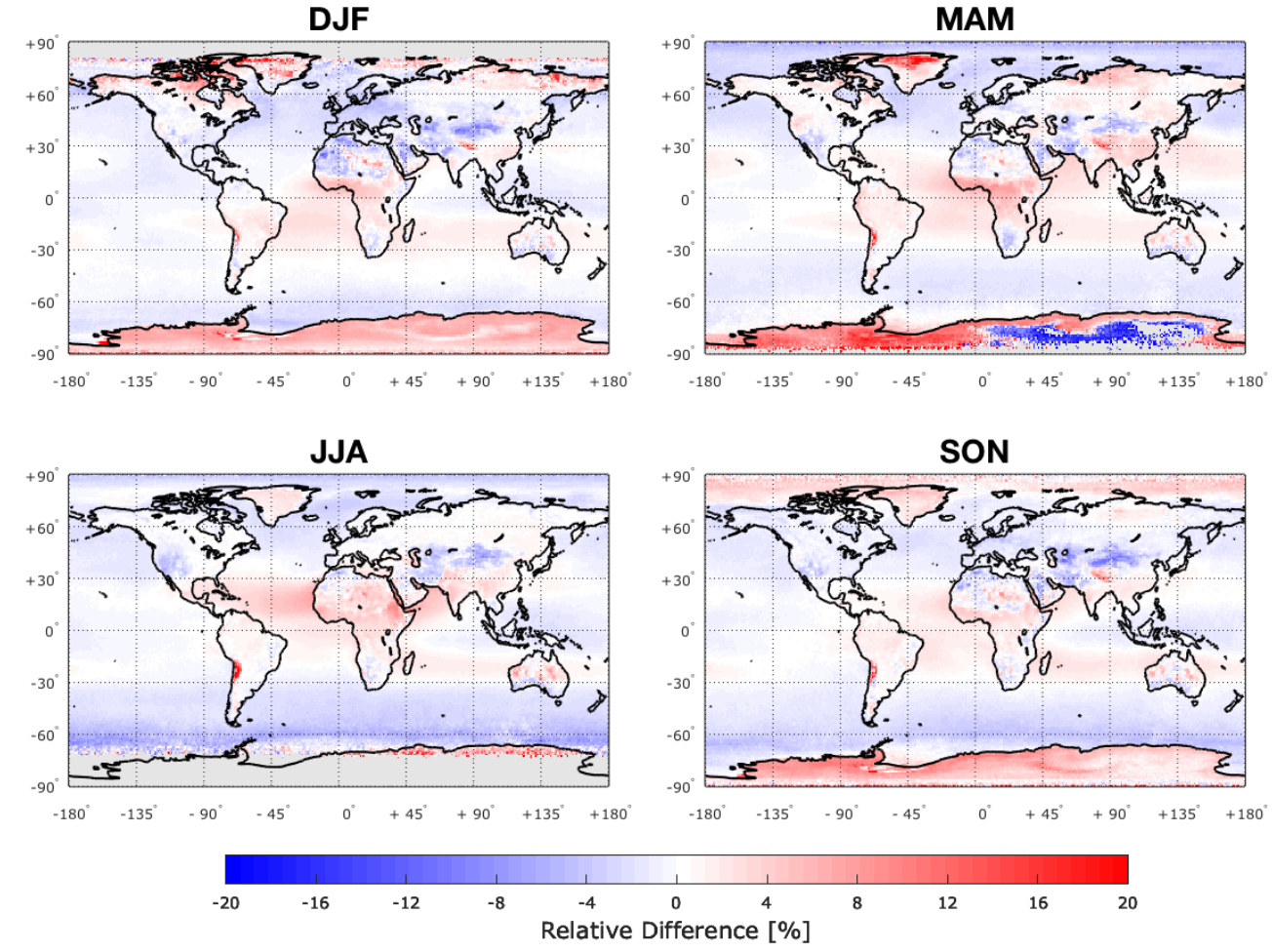

Figure 6: Seasonal distribution of the relative differences (in percent) between IASI-A and GOME-2A Total Ozone Column products for the period 2008 – 2017. The relative difference is calculated as 100 x (IASI-A-GOME-2A) / GOME-2A.

Atmos. Meas. Tech. Discuss., https://doi.org/10.5194/amt-2017-461
Manuscript under review for journal Atmos. Meas. Tech.
Discussion started: 22 January 2018

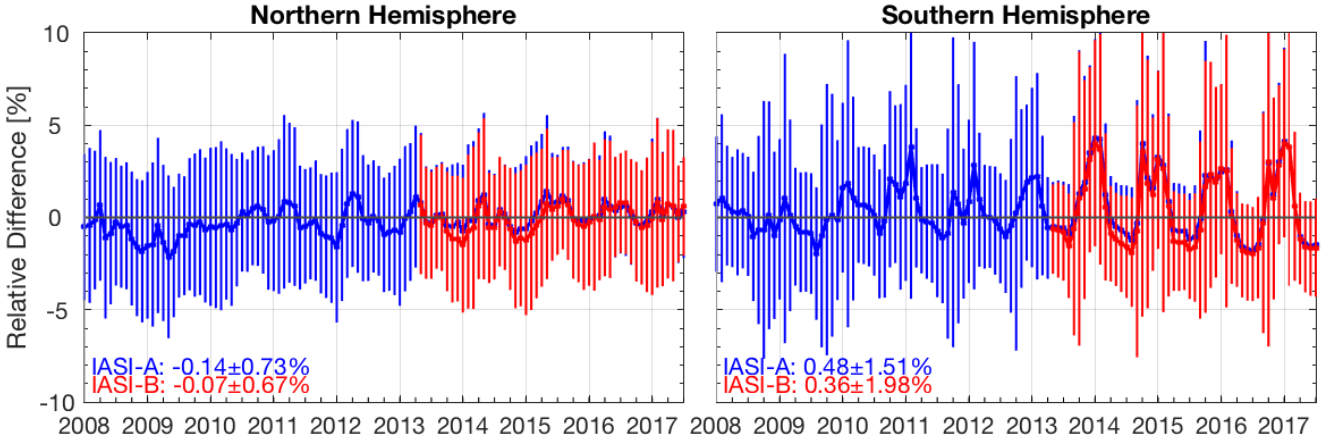

Figure 7: Monthly relative differences (in percent) between IASI-A (blue) and IASI-B (red) against GOME-2A Total Ozone Column products as a function of time for the period 2008 – 2017 for the Northern Hemisphere (left) and the Southern Hemisphere (right). The 1-sigma standard deviation of the relative differences is also displayed (vertical bars). Comparison statistics including mean biases and standard deviations in percent for the common period May 2013 – July 2017 are indicated on each panel.

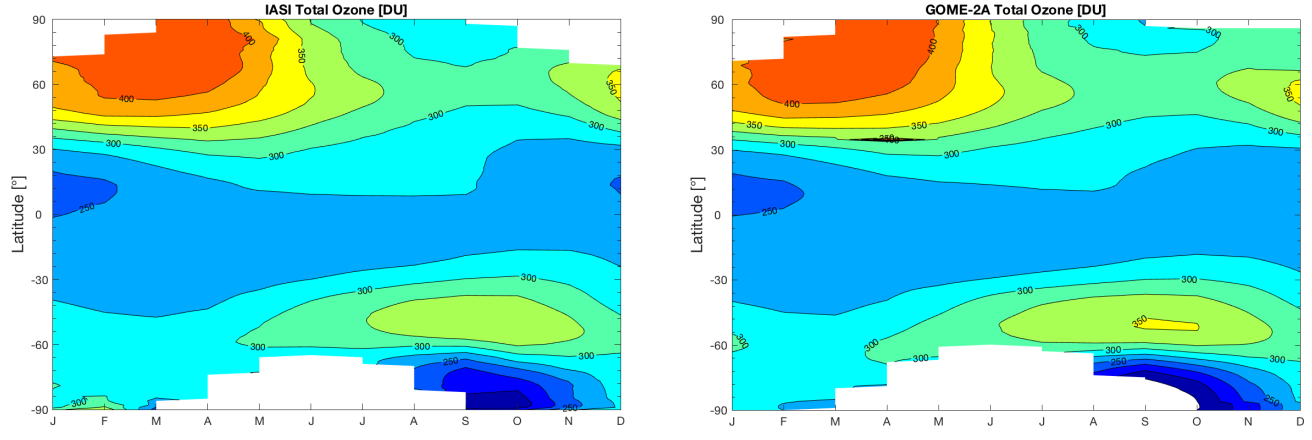

Figure 8: Latitude – season plot of daily 1°x1° Total Ozone Column products averaged for each month over the time period 2008 – 2017 for IASI-A (left) and GOME-2A (right).

Atmos. Meas. Tech. Discuss., https://doi.org/10.5194/amt-2017-461
Manuscript under review for journal Atmos. Meas. Tech.
Discussion started: 22 January 2018

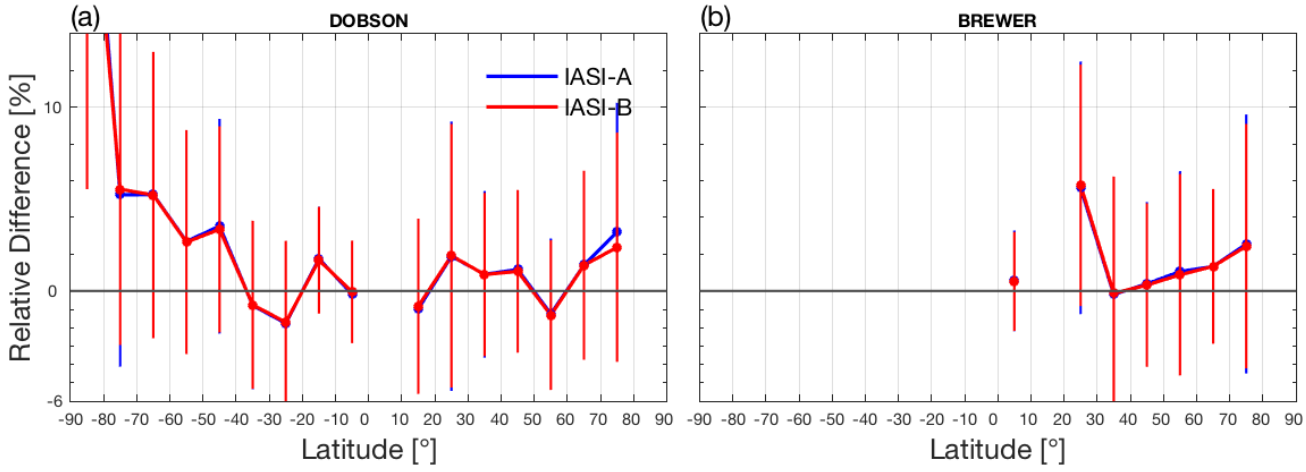

Figure 9: Latitudinal variability of the relative difference (in percent) between IASI-A (blue) and IASI-B (red) against collocated Dobson (left) and Brewer (right) TOC data given in bins of 10°. Only the common collocations between the two satellites are shown (period May 2013 – July 2017). The 1-sigma standard deviation of the relative differences is also displayed (vertical bars).

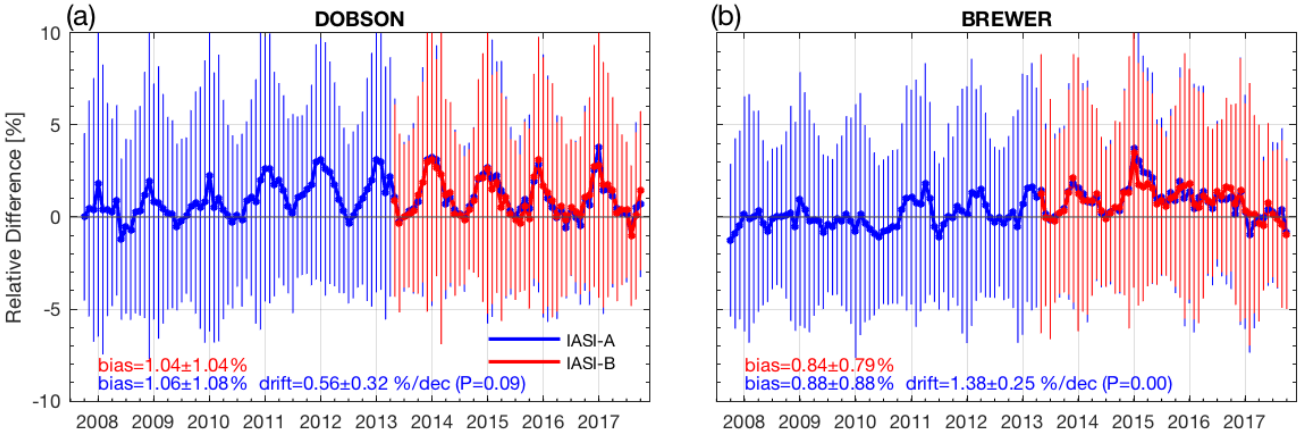

Figure 10: Time series of the monthly relative differences (in percent) between IASI-A (blue) and IASI-B (red) against collocated ground-based TOC for the Northern Hemisphere for the Dobson network (left) and Brewer network (right). For the period May 2013 onwards, only the common collocations between IASI-A and IASI-B are shown. The 1-sigma standard deviation of the average is also displayed (vertical bars). Comparison statistics including mean biases and standard deviations in percent for the common period May 2013 – July 2017 along with the decadal drift in percent and the *P* value for the IASI-A time series are indicated on each panel.

Atmos. Meas. Tech. Discuss., https://doi.org/10.5194/amt-2017-461
Manuscript under review for journal Atmos. Meas. Tech.
Discussion started: 22 January 2018

Atmospheric Measurement Techniques Discussions

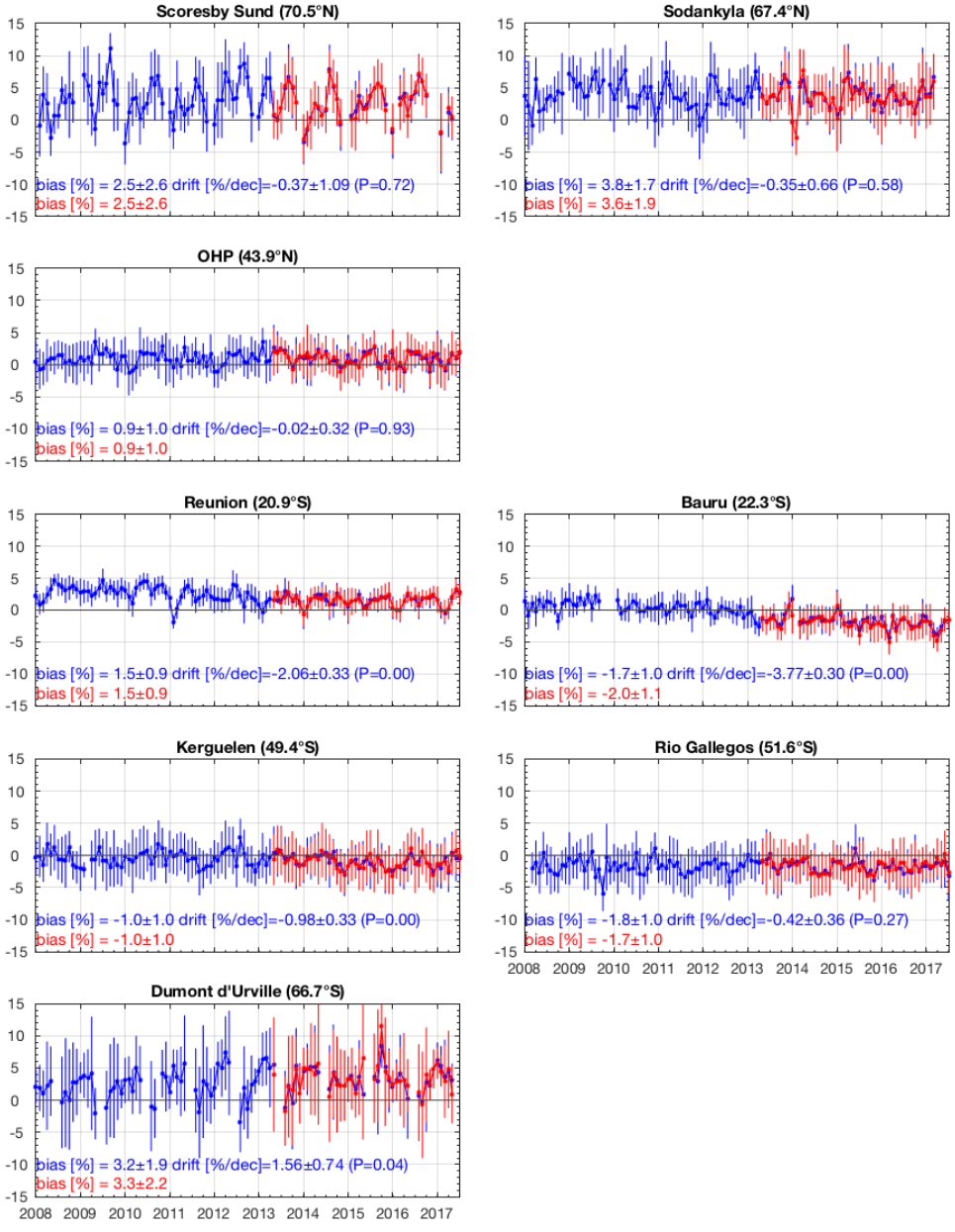

Figure 11: Time series of the monthly relative differences (in percent) between IASI-A (blue) and IASI-B (red) against collocated SAOZ TOC measurements for eight stations from North to South. For the period May 2013 onwards, only the common collocations between IASI-A and IASI-B are shown. The standard deviation of the average is also displayed (vertical bars). Comparison statistics including mean biases and standard deviations in percent for the common period May 2013 – July 2017, the decadal drift in percent and the *P* value for the IASI-A time series are indicated on each panel.

Atmos. Meas. Tech. Discuss., https://doi.org/10.5194/amt-2017-461
Manuscript under review for journal Atmos. Meas. Tech.
Discussion started: 22 January 2018

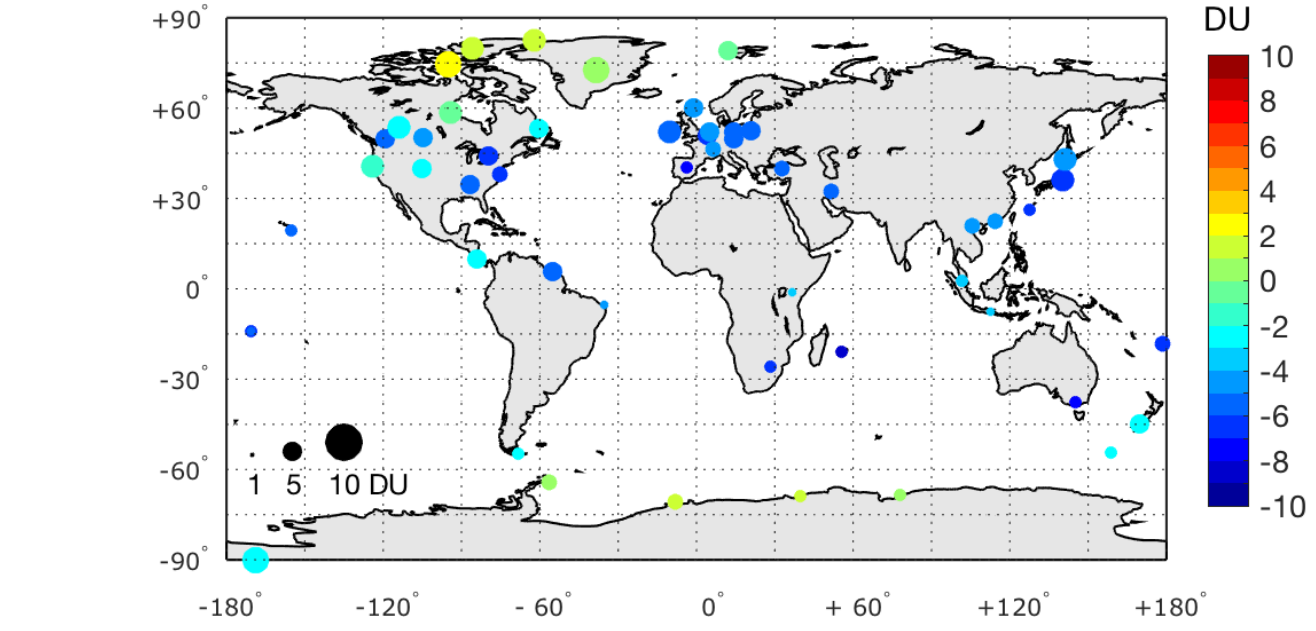

Figure 12: Spatial distribution of ozonesonde stations used in this study. The color represents the mean biases in Dobson Unit between IASI-A and ozonesonde TROPO O_3 columns (as defined as the surface-300 hPa column) at each station and the dot size represents the standard deviation. The average is performed for the period January 2008 – July 2017 only for the stations with more than 10 IASI-ozonesonde pairs.

Atmos. Meas. Tech. Discuss., https://doi.org/10.5194/amt-2017-461
Manuscript under review for journal Atmos. Meas. Tech.
Discussion started: 22 January 2018

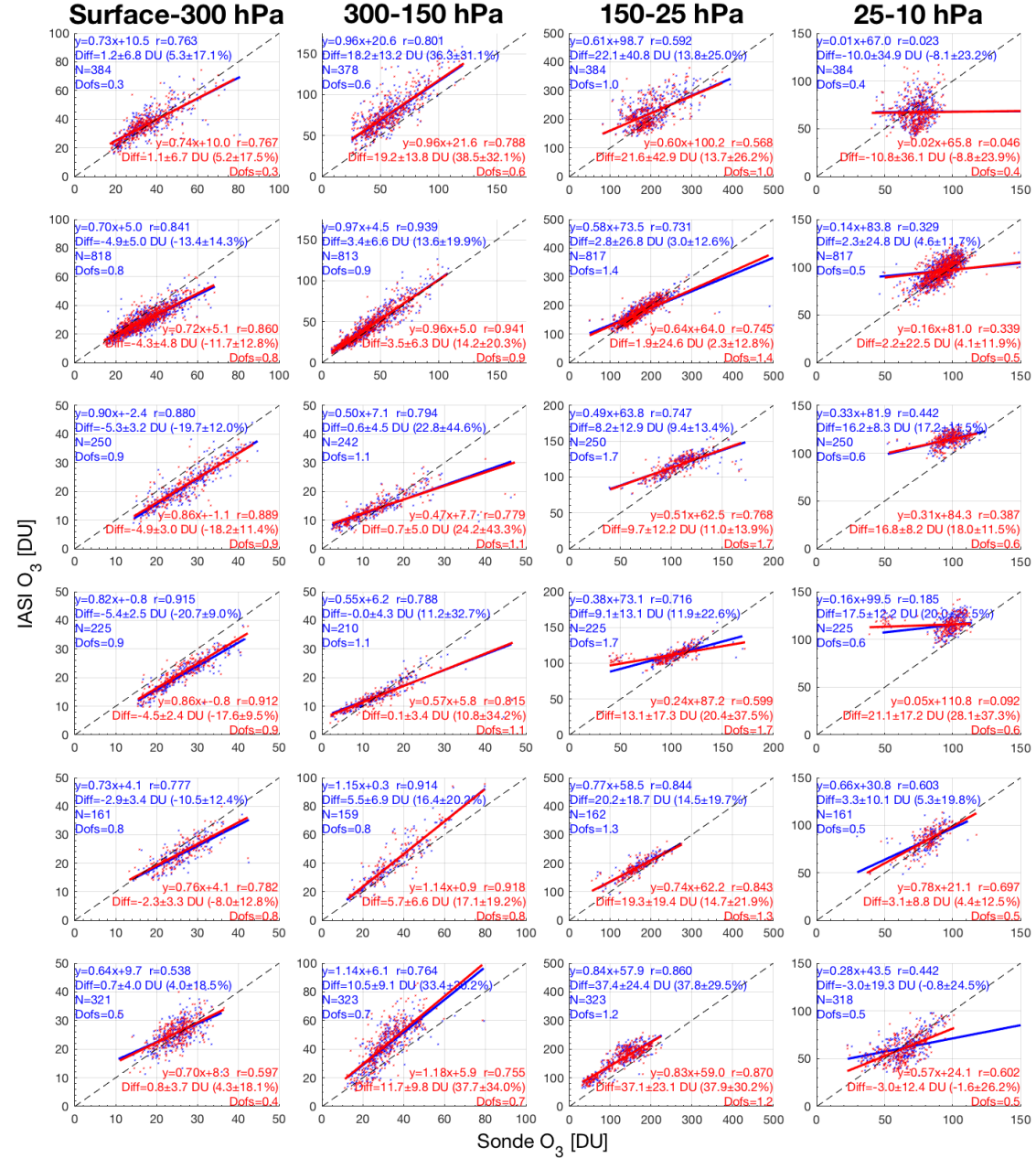

Figure 13: Scatter plots of collocated IASI-A (blue) and IASI-B (red) against smoothed ozonesonde O_3 sub-columns for six latitude bands for the common period May 2013 – July 2017. Comparison statistics including the linear regression, the mean differences and standard deviation in both Dobson Unit and percent, the number of collocations and the mean DOFS for each sub-column are shown on each panel.

Atmos. Meas. Tech. Discuss., https://doi.org/10.5194/amt-2017-461
Manuscript under review for journal Atmos. Meas. Tech.
Discussion started: 22 January 2018

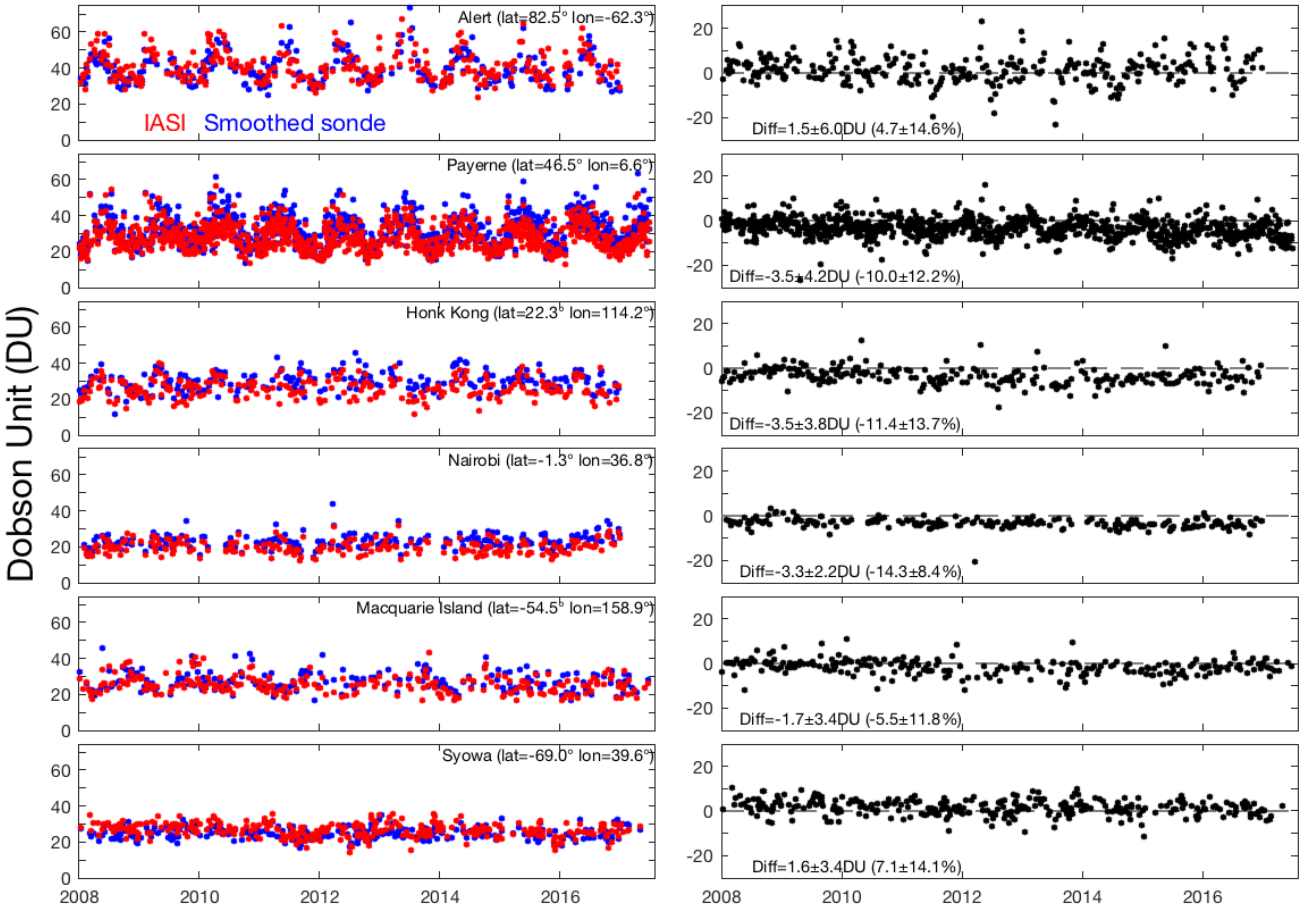

Figure 14: (left panels) Time series of daily IASI-A (in red) and smoothed ozonesonde (in blue) TROPO O_3 columns for six stations representative of different latitude bands for the period 2008 – 2017; (right panels) Associated relative differences (in percent), including the mean differences and 1-sigma standard deviation.

Atmos. Meas. Tech. Discuss., https://doi.org/10.5194/amt-2017-461
Manuscript under review for journal Atmos. Meas. Tech.
Discussion started: 22 January 2018

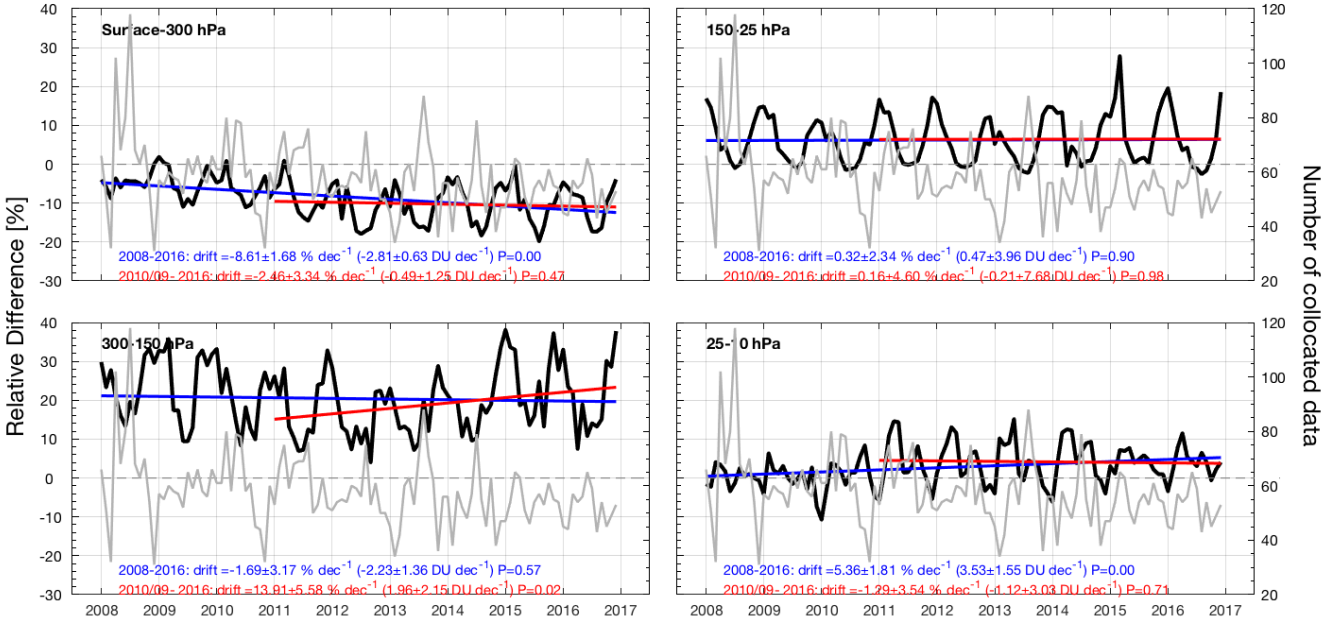

Figure 15: Time series of the monthly mean relative differences between IASI-A and ozonesonde O_3 measurements for different sub-columns for the period 2008 – 2017 for the Northern Hemisphere. The number of collocated data is also displayed in gray. The decadal drift in percent, the 1-sigma standard deviation and the *P* value are indicated on each panel for 2 periods: 2008 – 2016 (blue) and 2011 – 2016 (red).